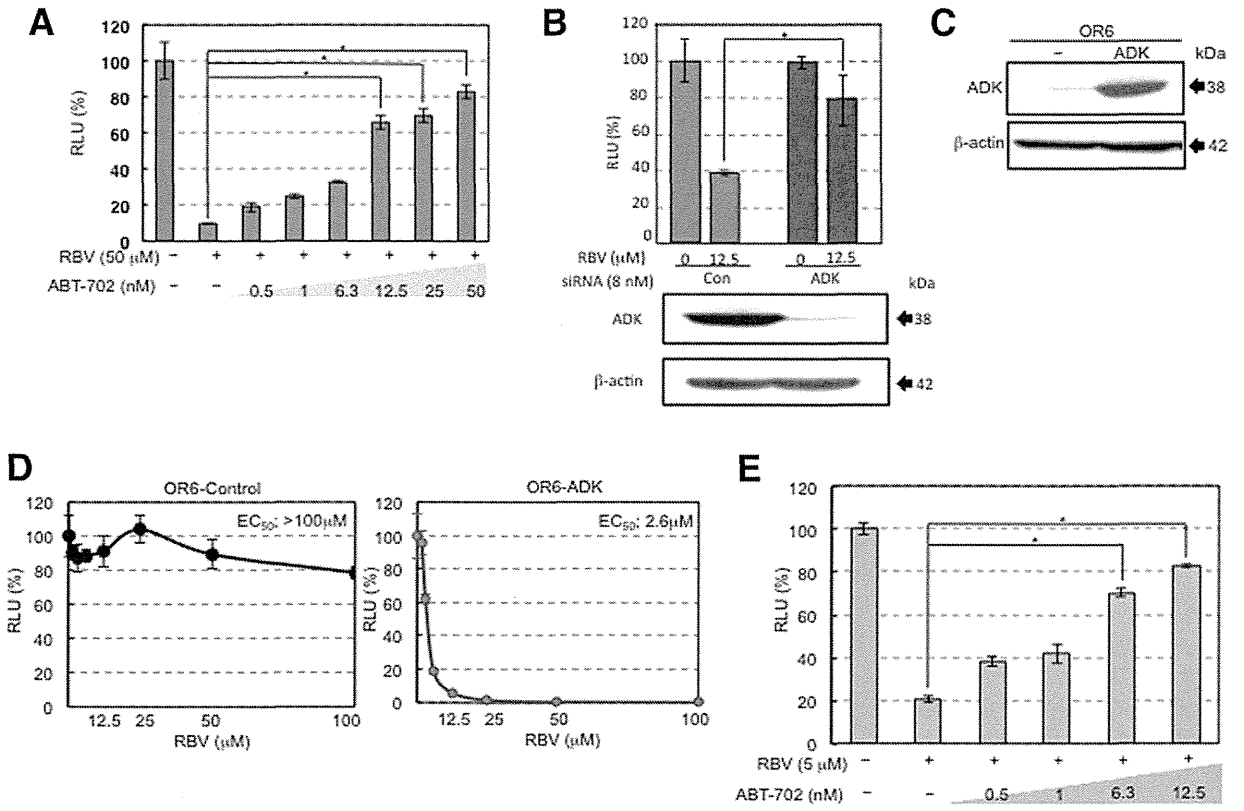

Fig. 2. ADK is a determining host factor for the anti-HCV activity of RBV. (A) ORL8 cells were cotreated with RBV (50 μM) and ABT-702 (nM) for 72 hours, after which an RL assay was performed. Relative luciferase activity (RLU) (%) calculated at each time point, when the level of luciferase activity in nontreated cells was assigned to be 100%, is shown. (B) ORL8 cells were transfected with 8 nM of siRNA targeting ADK. After 72 hours, expression levels of ADK were monitored by western blotting analysis (lower panel). ADK-knockdown ORL8 cells were treated with 12.5 μM of RBV for 72 hours, after which an RL assay was performed, as described in (A, upper panel). (C) Expression level of ADK in OR6-ADK cells was monitored by western blotting analysis. (D) OR6-ADK cells were treated with RBV for 72 hours and then an RL assay was performed as described in (A). (E) OR6-ADK cells were cotreated with RBV (5 μM) and ABT-702 (nM) for 72 hours and then an RL assay was performed, as described in (A). Experiments (A, B, D, and E) were performed in triplicate. $*P < 0.05$.

competitive inhibitor of IMPDH, by ADK.[16] Based on our findings, we expected that ADK activity might be able to control the anti-HCV activity of RBV. Indeed, microarray analysis revealed that the actual expression levels of ADK were 764 and 2,840 in OR6c and ORL8c cells, respectively. Quantitative RT-PCR analysis also showed that the mRNA level of ADK in ORL8 cells was 4.5 times higher than that in OR6 cells (Fig. 1C). Furthermore, we found that the protein level of ADK in ORL8 cells was much higher than that in OR6 cells (Fig. 1D).

On the other hand, it is known that ADK has two major isoforms: ADK-long (NM_006721) localized in the nucleus and ADK-short (NM_001123) localized in the cytoplasm.[17] ADK-long differs in the 5' UTR and initiates translation at an alternative start codon, compared to ADK-short. ADK-long is 17 amino acids longer than ADK-short. We prepared ORL8 cells stably overexpressing ORL8-derived ADK-long or ADK-short using a retroviral gene transfer system and examined its mobility in western blotting analysis. Fortunately, two isoforms were discriminable as 40 (ADK-long) and 38 kDa (ADK-short) (Fig. 1E). Using these isoforms as molecular markers, we performed semiquantitative western blotting analysis by the sample dilution method. The results revealed that the expression level of ADK-short in ORL8 cells was approximately 16 times higher than that in OR6 cells, and that ADK-long was little expressed in both cells (Fig. 1E). From these results, we assumed that the differences in ADK expression were involved in the dramatic differences in RBV sensitivity between the two cell lines. To address this assumption, we focused on the ADK-short in the following study; hereafter, ADK-short is designated as ADK.

ADK Is a Host Factor Determining the Anti-HCV Activity of RBV. To evaluate the hypothesis that ADK controls the anti-HCV activity of RBV, we first examined the effect of ABT-702, an ADK inhibitor, on the anti-HCV activity of RBV. The results revealed that ABT-702 cancelled the activity of RBV in ORL8

cells in a dose-dependent manner (Fig. 2A). Furthermore, we demonstrated that the activity of RBV was cancelled in ADK-knockdown ORL8 cells (Fig. 2B). These results suggest that the inhibition of ADK in ORL8 cells converts them from an RBV-sensitive phenotype to an RBV-resistant phenotype.

To directly demonstrate the involvement of ADK, we first prepared OR6 cells stably expressing ADK (OR6-ADK) (Fig. 2C). We were able to demonstrate that the OR6-ADK cells were dramatically converted from an RBV-resistant phenotype with an EC_{50} value of more than 100 μM to an RBV-sensitive phenotype with an EC_{50} value of 2.6 μM (Fig. 2D). We next examined whether or not the GTP reduction or IMP accumulation observed in ORL8 cells treated with RBV (Fig. 1A,B) occurs in OR6-ADK cells. The results revealed that the GTP reduction and IMP accumulation in RBV-treated OR6-ADK cells were more pronounced than in RBV-treated ORL8 cells (Supporting Fig. 3A,B). Because OR6 is a clonal cell line harboring genome-length HCV RNA, we used a polyclonal cell line (sOR) harboring HCV replicon RNA[9] to prepare sOR-ADK cells stably expressing ADK (Supporting Fig. 3C) and examined their sensitivity to RBV. sOR-ADK cells were also dramatically converted from an RBV-resistant phenotype with an EC_{50} value of more than 100 μM to an RBV-sensitive phenotype with an EC_{50} value of 6.0 μM (Supporting Fig. 3D). In addition, ORL8-ADK cells stably overexpressing ADK also showed EC_{50} values ranging from 13.2 to 1.2 μM (Supporting Fig. 3E). Furthermore, we demonstrated that the anti-HCV activity detected in OR6-ADK cells was also cancelled by ABT-702 treatment in a dose-dependent manner (Fig. 2E). Considering these results together, we conclude that ADK is a key determinant for the anti-HCV activity of RBV.

The Suppression of ADK Expression in OR6 Cells Was Not the Result of Genetic Variations or Epigenetic Alterations in the ADK Gene Promoter. To clarify the mechanism underlying the difference in ADK expression between OR6 and ORL8 cells, we first examined the nt sequences of up to several kb upstream from the transcription start point estimated from NM_001123 (31-OCT-2010) using the data of AL731576. Several possible transcription elements, such as the GC box (−12 and −187 of ADK gene), p53 response element (−252 and −585), and heat shock element (−559, −971, −1486, and −1797) were detected in up to approximately 2 kb upstream from the estimated transcription start point, but not in more 2 kb. Accordingly, we amplified approximately 2 kb including the 5' UTR (187 nts estimated by NM_001123 [31-OCT-2010]) by PCR using DNA prepared from ORL8 or OR6 cells, and each PCR product was inserted into pGL4.10-luc2 for the sequence analysis and reporter analysis of gene promoter activity. Sequence analysis confirmed that the sequences of the inserts were the same as the sequence data of the ADK gene (AL731576), except in the case of a single-nucleotide polymorphism (SNP) [rs10824095; C for ORL8 cells and T for OR6 cells] located 20 bases upstream from the initiation codon. Luciferase reporter assay using ORL8c cells revealed that the promoter activity of OR6 origin was almost equal to that of ORL8 origin (Supporting Fig. 4A), indicating that the detected SNP was not involved in the level of promoter activity.

We next evaluated the epigenetic effects on ADK expression level. The results revealed that the expression level of ADK mRNA in OR6 cells was not enhanced in the cells treated with 5azaC and/or 4-PBA for 48 hours (Supporting Fig. 4B). Moreover, the protein level of ADK was not increased in the OR6 cells treated with 5azaC for 6 days (Supporting Fig. 4C). Taken together, these results suggest that the low level of ADK mRNA in OR6 cells was not the result of genetic polymorphisms or epigenetic alternations in the ADK gene promoter region.

The Differential ADK Expression Between OR6 and ORL8 Cells Was Not Mediated by a microRNA Control Mechanism. To explain the above-described gap between the 4.5-fold difference in the mRNA level and the 16-fold difference in the protein level (Fig. 1C,E), we hypothesized that the 3' UTR of ADK mRNA was different in the length or nt sequences between OR6 and ORL8 cells, and that such differences affected the control mechanism by microRNA (miRNA). To test this hypothesis, we first performed 3' rapid amplification of cDNA ends (RACE) analysis on ADK mRNA using total RNA prepared from OR6 or ORL8 cells. Sequence analysis using more than 45 cDNA clones obtained from each cell line was carried out. 3' UTRs of four different lengths were detected in both OR6 and ORL8 cells, because four potential poly(A) additional signals were present in the downstream ADK open reading frame (ORF) (Supporting Fig. 5). The results revealed no qualitative difference of 3' UTR species between OR6 and ORL8 cells (Supporting Fig. 5).

Because the 3' UTR of ADK mRNA contained the seed sequences of miR-182, miR-203, mir-125a-3p, and miR-106b (Supporting Fig. 5), we assumed that

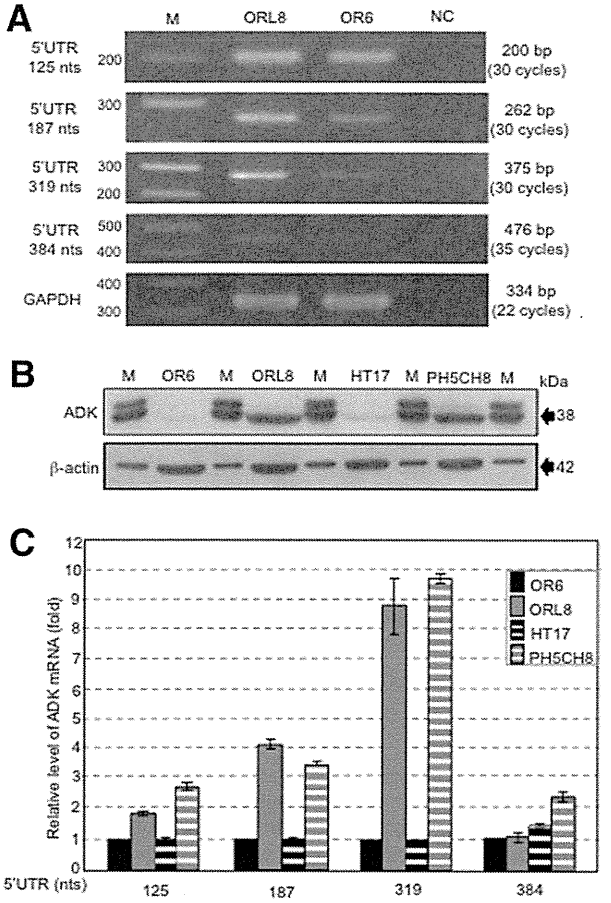

Fig. 3. Level of ADK mRNA possessing long 5' UTR was correlated with the expression level of ADK. (A) Total RNAs prepared from ORL8 and OR6 cells were subjected to RT-PCR using the primer sets (Supporting Table 1) for various lengths of 5' UTR of ADK mRNA. (B) Expression levels of ADK were compared by western blotting analysis. The two molecular markers of ADK shown in Fig. 1E were loaded on every two lanes. (C) Amounts of 5' UTR species of ADK mRNAs were compared by quantitative RT-PCR analysis using the primer sets described in (A). Experiments were performed in triplicate.

the difference in expression levels of these miRNAs causes the different protein levels of ADK. To examine this possibility, we performed an miRNA microarray analysis between OR6 and ORL8 cells. This analysis revealed very low expression levels (measured values of less than 7) of miR-182, miR203, and miR-125a-3p in both cell lines. Although only miR-106b was moderately expressed (measured value of approximately 300) in OR6 and ORL8 cells, the values obtained from both cell lines were almost the same. From these results, these miRNAs may not participate in the translational regulation of ADK mRNAs in OR6 and ORL8 cells.

The 5' UTR of ADK mRNA in ORL8 Cells Was Longer Than That in OR6 Cells. To explain the dramatic difference in ADK expression between ORL8 and OR6 cells, we next focused on the 5' UTR. To date, two different lengths of 5' UTR (384 nts in accession number NM_001123[25-MAR-2011] and 187 nts in accession numbers NM_001123[31-OCT-2010] and HSU_50196) have been deposited in GeneBank. Because the 384 nts form has been considered to be a unique species in testis tissue, we performed 5' RACE analysis to determine the length of the 5' UTR of ADK mRNA in ORL8 or OR6 cells. Sequence analysis was carried out using more than 20 cDNA clones obtained from each cell line. Consequently, we obtained 319 and 125 nts as the major 5' UTR species in ORL8 and OR6 cells, respectively. We confirmed these results by RT-PCR analysis using four different primer sets for the 5' UTR (Fig. 3A). The amount of 384 nts species in ORL8 cells was estimated to be less than one thirtieth the amount of the 319-nts species (Fig. 3A). These results indicate that the length of 5' UTR in ORL8 cells is longer than that in OR6 cells.

From these results, we considered the possibility that the length of the 5' UTR is associated with the protein level of ADK. To test this possibility, we first compared the expression levels of ADK in various human hepatoma cell lines and human immortalized hepatocyte lines. Low expression level of ADK was observed in HT17 and Hep3B cells as well as OR6 cells, although the other cell lines, including ORL8, HuH-6, HepG2, HLE, and PH5CH8 cells, showed high expression level of ADK (Fig. 3B and Supporting Fig. 6). We next performed quantitative RT-PCR analysis on the 5' UTR using total RNAs from OR6, ORL8, HT17, and PH5CH8 cells. Consequently, we found that the 319 nts species of the 5' UTR was abundant in PH5CH8 cells, but not in HT17 cells (Fig. 3C), indicating good correlation between the amount of 319 nts species and the amount of ADK protein (Fig. 3B,C). These results suggest that the 319 nts species of 5' UTR is involved in the high protein level of ADK.

The Long-Form 5' UTR of ADK mRNA Possessed IRES Activity. From the results of 5' UTR analysis, we assumed that the 319 nts species of the 5' UTR possesses IRES activity because it is GC rich (72%) and highly structured (estimated $\Delta G = -110.7$ kcal/mol), and because it contains an upstream ORF for 70 amino acids. To test this assumption, we used a bicistronic dual luciferase reporter assay system for the detection of IRES activity (Fig. 4A). As a positive control, we constructed a pGL4-based reporter plasmid containing HCV IRES (377 nts; 341 nts in the 5' UTR plus the first 36 nts in the Core-encoding

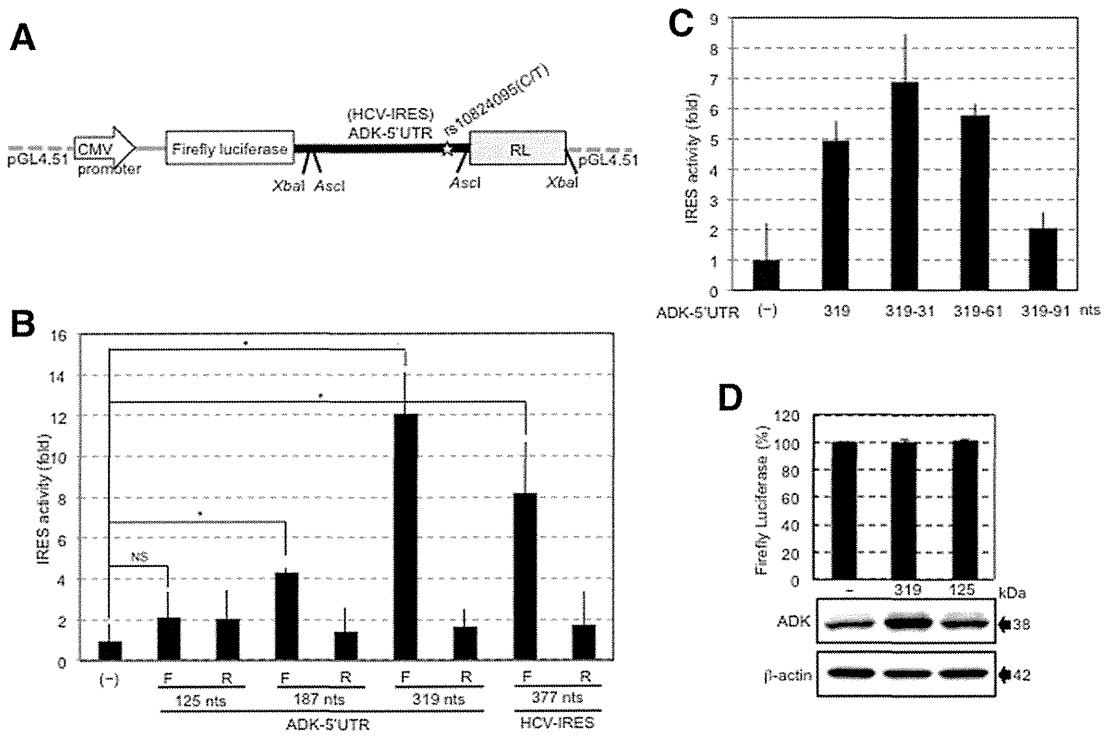

Fig. 4. Long-form 5' UTR of ADK mRNA possessed IRES activity. (A) Partial structure of the plasmid used as a dicistronic dual reporter assay system. (B) ORL8c cells were transfected with the plasmid as shown in (A). After 48 hours, a dual luciferase assay was performed. The ratio of the RL activity to firefly luciferase activity was calculated. The relative value calculated at each sample, when the ratio in the control vector-transfected cells (−) was assigned to be 1, is presented. F and R indicate the forward and reverse direction of insert in the reporter plasmid, respectively. (C) Deletion mutant analysis of the 5' UTR in IRES assay. IRES assay was performed using ORL8c cells transfected with the reporter plasmid containing the deleted forms of the 5' UTR, as described in (B). (D) ADK expression derived from the long-form 5' UTR transcript was more productive than that from the short-form 5' UTR transcript. OR6c cells were transfected with the plasmid, in which the *Xba*I fragment of the plasmid used for HCV IRES activity assay was replaced by the ADK ORF possessing the 5' UTR of 319 or 125 nts. After 48 hours, western blotting analysis was performed. Firefly luciferase activities were measured to check equal transfection efficiency. Experiments (B and C) were performed in triplicate. $*P < 0.05$; NS, not significant.

region). We next replaced the HCV IRES structure in this plasmid with several different lengths (forward or reverse direction) of the 5' UTR derived from ORL8 cells. ORL8c cells were transfected with these plasmids, and at 48 hours after transfection, dual luciferase assays were performed. Consequently, we found that the forward 319 nts, but not the forward 125 nts, of 5' UTR clearly showed IRES activity at the same level as HCV IRES (Fig. 4B). The 187 nts species also showed weak IRES activity (Fig. 4B). None of the 5' UTR species with reverse direction and none of the HCV IRES with reverse direction showed any IRES activities (Fig. 4B). Furthermore, similar results were obtained in the genome-length HCV RNA-replicating OL8 cells and their cured cells (OL8c) (Supporting Fig. 7A,B), suggesting that IRES activity does not depend on cell strains or HCV RNA replication. In addition, we did not observe any effects of an SNP (rs10824095), which was located 20 bases upstream from the initiation codon, on the IRES activities of OR6 and ORL8 cell-derived 5' UTRs (319 nts) (Supporting Fig. 8).

To identify the entry site of the 40S ribosome in the IRES region, we prepared three deletion mutants (deleted upstream 30, 60, and 90 nts from the initiation codon) of the 5' UTR and measured their IRES activities in ORL8c cells. The results revealed that the deletion up to 60 nts from the initiation codon did not decrease IRES activity, but the 90 nts deletion abolished IRES activity (Fig. 4C). Similar results were also obtained in OL8 and OL8c cells (Supporting Fig. 7C,D). These results suggest that the entry site of the 40S ribosome is between 60 and 90 nts upstream from the initiation codon, and that the region from 319 to 61 nts upstream from the initiation codon is necessary for the IRES activity. It is noteworthy that this region forms a stable secondary structure (estimated $\Delta G = -108.4$ kcal/mol) (Supporting Fig. 7E). Furthermore, we demonstrated that ADK expression derived from the long-form 5' UTR transcript was

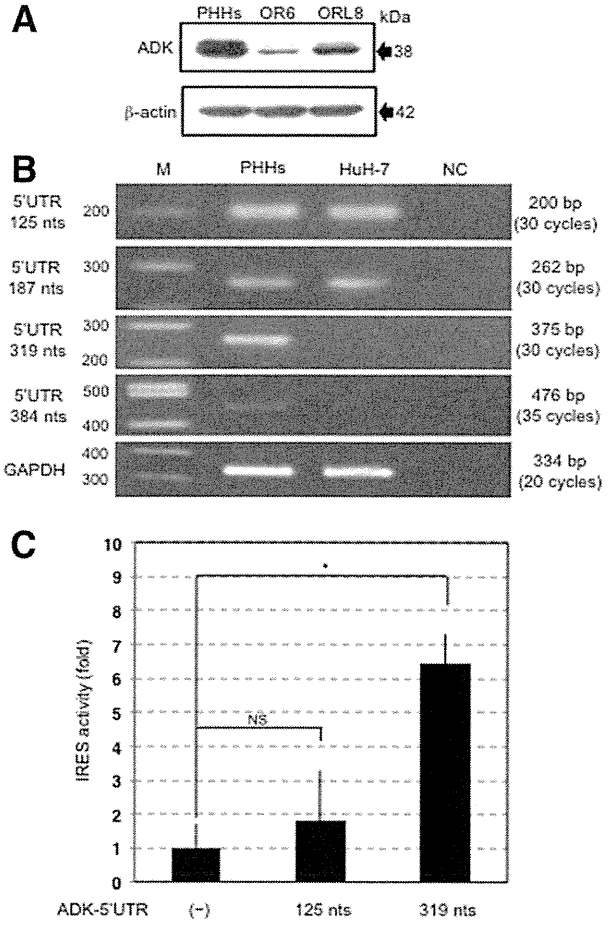

Fig. 5. Long-form 5' UTR of ADK mRNA functioned as an IRES in PHHs. (A) ADK expression level in PHHs was compared with those in OR6 and ORL8 cells by western blotting analysis. (B) Total RNAs prepared from PHHs and HuH-7 cells were subjected to RT-PCR analysis using the primer sets described in Fig. 3A. (C) PHHs were transfected with the plasmid shown in Fig. 4A. After 48 hours, a dual luciferase assay was performed as described in Fig. 4B. Experiments (B and C) were performed in triplicate. $*P < 0.05$; NS, not significant.

more productive than the expression from the short-form 5' UTR transcript in OR6c cells (Fig. 4D).

The Long-Form 5' UTR of ADK mRNA Functioned as an IRES in Primary Human Hepatocytes. To obtain a final conclusion, we examined whether the novel mechanism in ADK translation plays a role in PHHs. We first examined ADK expression level in PHHs, and the results revealed that ADK protein level was higher in PHHs than in ORL8 cells (Fig. 5A). We next performed RT-PCR analysis using the primer sets used in Fig. 3A to examine the amounts of 319 and 125 nts forms of the 5' UTR. The results showed that the 319 nts species was the major 5' UTR species in PHHs, but not in HuH-7 cells, which are the parent of OR6 cells (Fig. 5B), indicating a good correlation between the amount of 319 nts species and the amount of ADK protein in PHHs. Finally, we demonstrated that the 319 nts form, but not the 125 nts form, of 5' UTR clearly showed IRES activity in PHHs (Fig. 5C).

Considering all these results together, we conclude that not only ORL8 cells, but also PHHs express the long-form 5' UTR of ADK mRNA possessing IRES activity and then produce high levels of ADK, which works as an RBV kinase.

Discussion

In this study, we identified, for the first time, a host factor ADK whose expression level could control the anti-HCV activity of RBV. Furthermore, we found that the expression level of ADK was associated with the amount of ADK mRNA possessing long 5' UTR exhibiting IRES activity. This finding suggests that the RBV sensitivity on HCV RNA replication is regulated by the IRES-dependent translation of ADK mRNA. If ADK expression levels or activity differ between patients with CHC, it may be a useful therapeutic target.

It has recently been reported that a functional SNP (rs1127354; major C and minor A) in inosine triphosphatase was the most significant SNP associated with RBV-induced anemia.[18] In this context, we hypothesized that this SNP is associated with the expression level of ADK. To test this hypothesis, we examined the status of rs1127354 in ORL8 and PH5CH8 cells showing high expression levels of ADK and in OR6 and Hep3B cells showing low expression levels of ADK. The results revealed that all cell lines showed the major C of the SNP, suggesting that rs1127354 is not associated with the expression level of ADK.

The most striking highlight in this study is the IRES activity found in ADK mRNA. It has recently been reported that cellular IRES-mediated translation is activated by many physiological and pathological stress conditions in eukaryotic cells.[19] To achieve efficient IRES-dependent translation, some triggers will be needed. However, HCV RNA replication was not such a trigger, in the present study, because a similar level of IRES activity was observed in both OL8c cured cells and genome-length HCV RNA-replicating OL8 cells (Supporting Fig. 7A-D). The addition of adenosine did not act as a trigger for IRES (Supporting Fig. 9). Another possible explanation for the high level of ADK in ORL8 cells would be the involvement of one or more miRNA(s) in stabilizing the IRES-containing ADK mRNA, as reported in HCV RNA.[20] To test this possibility, we performed comparative miRNA microarray analysis using ORL8, PH5CH8, OR6, and HT17 cells. The results revealed that nts 1-8 of miR-

424, whose expression levels in ORL8 and PH5CH8 cells were several times higher than those in OR6 and HT17 cells, showed base pairs in the nt 61-68 upstream initiation codon of ADK mRNA. It was noticed that this region in ADK mRNA overlaps the region (nt 60-90 upstream initiation codon of ADK mRNA) identified as the entry site of the 40S ribosome. However, a preliminary experiment showed that overexpression of miR-424 in ORL8 or OR6 cells did not enhance the translation of ADK (Supporting Fig. 10), suggesting that miR-424 is not associated with the high level of ADK in ORL8 cells. The possibility remains that other miRNA(s) participate in the up-regulation of ADK.

At this time, we have identified ADK as a host factor that controls the anti-HCV activity of RBV and clarified the molecular mechanism underlying regulation with ADK. Furthermore, we demonstrated that such a novel mechanism plays a role in PHHs. From our finding, we suggest that ADK expression is artfully regulated both at the transcription and translation stage. Although we identified ADK, which participates in nucleotidic metabolism, as an enzyme functionally controlled by the specific expression of an IRES-containing mRNA, there may be other gene products controlled by a similar mechanism.

Acknowledgments: The authors thank Naoko Kawahara, Takashi Nakamura, and Keiko Takeshita for their technical assistance.

References

1. Lindenbach BD, Rice CM. Unravelling hepatitis C virus replication from genome to function. Nature 2005;436:933-893.
2. Ghany MG, Nelson DR, Strader DB, Thomas DL, Seeff LB. An update on treatment of genotype 1 chronic hepatitis C virus infection: 2011 practice guideline by the American Association for the Study of Liver Diseases. HEPATOLOGY 2011;54:1433-1444.
3. Jacobson IM, McHutchison JG, Dusheiko G, Di Bisceglie AM, Reddy KR, Bzowej NH, et al. Telaprevir for previously untreated chronic hepatitis C virus infection. N Engl J Med 2011;364:2405-2416.
4. Poordad F, McCone J, Jr., Bacon BR Bruno S, Manns MP, Sulkowski MS, et al. Boceprevir for untreated chronic HCV genotype 1 infection. N Engl J Med 2011;364:1195-1206.
5. Feld JJ, Hoofnagle JH. Mechanism of action of interferon and ribavirin in treatment of hepatitis C. Nature 2005;436:967-972.
6. Paeshuyse J, Dallmeier K, Neyts J. Ribavirin for the treatment of chronic hepatitis C virus infection: a review of the proposed mechanisms of action. Curr Opin Virol 2011;1:590-598.
7. Thomas E, Feld JJ, Li Q, Hu Z, Fried MW, Liang TJ. Ribavirin potentiates interferon action by augmenting interferon-stimulated gene induction in hepatitis C virus cell culture models. HEPATOLOGY 2011;53:32-41.
8. Zhou S, Liu R, Baroudy BM, Malcolm BA, Reyes GR. The effect of ribavirin and IMPDH inhibitors on hepatitis C virus subgenomic replicon RNA. Virology 2003;310:333-342.
9. Ikeda M, Abe K, Dansako H, Nakamura T, Naka K, Kato N. Efficient replication of a full-length hepatitis C virus genome, strain O, in cell culture, and development of a luciferase reporter system. Biochem Biophys Res Commun 2005;329:1350-1359.
10. Mori K, Ikeda M, Ariumi Y, Dansako H, Wakita T, Kato N. Mechanism of action of ribavirin in a novel hepatitis C virus replication cell system. Virus Res 2011;157:61-70.
11. Kato N, Mori K, Abe K, Dansako H, Kuroki M, Ariumi Y, et al. Efficient replication systems for hepatitis C virus using a new human hepatoma cell line. Virus Res 2009;146:41-50.
12. Mori K, Ikeda M, Ariumi Y, Kato N. Gene expression profile of Li23, a new human hepatoma cell line that enables robust hepatitis C virus replication: comparison with HuH-7 and other hepatic cell lines. Hepatol Res 2010;40:1248-1253.
13. Kato N, Sugiyama K, Namba K, Dansako H, Nakamura T, Takami M, et al. Establishment of a hepatitis C virus subgenomic replicon derived from human hepatocytes infected in vitro. Biochem Biophys Res Commun 2003;306:756-766.
14. Dansako H, Naganuma A, Nakamura T, Ikeda F, Nozaki A, Kato N. Differential activation of interferon-inducible genes by hepatitis C virus core protein mediated by interferon stimulated response element. Virus Res 2003;97:17-30.
15. Takatori S, Kanda H, Takenaka K, Wataya Y, Matsuda A, Fukushima M, et al. Antitumor mechanisms and metabolism of the novel antitumor nucleoside analogues, 1-(3-C-ethynyl-beta-D-ribo-pentofuranosyl)-cytosine and 1-(3-C-ethynyl-beta-D-ribo-pentofuranosyl)uracil. Cancer Chemother Pharmacol 1999;44:97-104.
16. Streeter DG, Witkowski JT, Khare GP, Sidwell RW, Bauer RJ, Robins RK, Simon LN. Mechanism of action of 1-β-D-ribofuranosyl-1,2,4-triazole-3-carboxamide (Virazole), a new broad-spectrum antiviral agent. Proc Natl Acad Sci U S A 1973;70:1174-1178.
17. Cui XA, Singh B, Park J, Gupta RS. Subcellular localization of adenosine kinase in mammalian cells: the long isoform of AdK is localized in the nucleus. Biochem Biophys Res Commun 2009;388:46-50.
18. Fellay J, Thompson AJ, Ge D, Gumbs CE, Urban TJ, Shianna KV, et al. ITPA gene variants protect against anaemia in patients treated for chronic hepatitis C. Nature 2010;464:405-408.
19. Komar AA, Hatzoglou M. Cellular IRES-mediated translation: the war of ITAFs in pathophysiological states. Cell Cycle 2011;10:229-240.
20. Shimakami T, Yamane D, Jangra RK, Kempf BJ, Spaniel C, Barton DJ, Lemon SM. Stabilization of hepatitis C virus RNA by an Ago2-miR-122 complex. Proc Natl Acad Sci U S A 2012;109:941-946.

PLOS ONE

New Preclinical Antimalarial Drugs Potently Inhibit Hepatitis C Virus Genotype 1b RNA Replication

Youki Ueda[1], Midori Takeda[1], Kyoko Mori[1], Hiromichi Dansako[1], Takaji Wakita[2], Hye-Sook Kim[3], Akira Sato[3], Yusuke Wataya[3], Masanori Ikeda[1], Nobuyuki Kato[1]*

1 Department of Tumor Virology, Okayama University Graduate School of Medicine, Dentistry, and Pharmaceutical Sciences, Shikata-cho, Okayama, Japan, **2** Department of Virology II, National Institute of Infectious Disease, Toyama, Shinjuku-ku, Tokyo, Japan, **3** Department of Drug Informatics, Faculty of Pharmaceutical Sciences, Okayama University, Tsushima-naka, Okayama, Japan

Abstract

Background: Persistent hepatitis C virus (HCV) infection causes chronic liver diseases and is a global health problem. Although new triple therapy (pegylated-interferon, ribavirin, and telaprevir/boceprevir) has recently been started and is expected to achieve a sustained virologic response of more than 70% in HCV genotype 1 patients, there are several problems to be resolved, including skin rash/ageusia and advanced anemia. Thus a new type of anti-HCV drug is still needed.

Methodology/Principal Findings: Recently developed HCV drug assay systems using HCV-RNA-replicating cells (e.g., HuH-7-derived OR6 and Li23-derived ORL8) were used to evaluate the anti-HCV activity of drug candidates. During the course of the evaluation of anti-HCV candidates, we unexpectedly found that two preclinical antimalarial drugs (N-89 and its derivative N-251) showed potent anti-HCV activities at tens of nanomolar concentrations irrespective of the cell lines and HCV strains of genotype 1b. We confirmed that replication of authentic HCV-RNA was inhibited by these drugs. Interestingly, however, this anti-HCV activity did not work for JFH-1 strain of genotype 2a. We demonstrated that HCV-RNA-replicating cells were cured by treatment with only N-89. A comparative time course assay using N-89 and interferon-α demonstrated that N-89-treated ORL8 cells had more rapid anti-HCV kinetics than did interferon-α-treated cells. This anti-HCV activity was largely canceled by vitamin E. In combination with interferon-α and/or ribavirin, N-89 or N-251 exhibited a synergistic inhibitory effect.

Conclusions/Significance: We found that the preclinical antimalarial drugs N-89 and N-251 exhibited very fast and potent anti-HCV activities using cell-based HCV-RNA-replication assay systems. N-89 and N-251 may be useful as a new type of anti-HCV reagents when used singly or in combination with interferon and/or ribavirin.

Citation: Ueda Y, Takeda M, Mori K, Dansako H, Wakita T, et al. (2013) New Preclinical Antimalarial Drugs Potently Inhibit Hepatitis C Virus Genotype 1b RNA Replication. PLoS ONE 8(8): e72519. doi:10.1371/journal.pone.0072519

Editor: Hak Hotta, Kobe University, Japan

Received April 11, 2013; **Accepted** July 5, 2013; **Published** August 30, 2013

Funding: This study was supported by a grant-in-aid for research on hepatitis from the Ministry of Health, Labor and Welfare of Japan. The funders had no role in study design, data collection and analysis, decision to publish, or preparation of the manuscript.

Competing Interests: The authors have declared that no competing interests exist.

* E-mail: nkato@md.okayama-u.ac.jp

Introduction

Hepatitis C virus (HCV) infection causes chronic hepatitis, which can lead to liver cirrhosis and hepatocellular carcinoma. Approximately 170 million people are infected with HCV worldwide, making HCV infection a serious global health problem [1]. HCV is an enveloped virus with a positive single-stranded RNA genome, and belongs to the *Flaviviridae* family. The HCV genome encodes a large polyprotein precursor of approximately 3000 amino acids, which is cleaved into 10 proteins in the following order: Core, envelope 1 (E1), E2, p7, non-structural 2 (NS2), NS3, NS4A, NS4B, NS5A, and NS5B [2,3].

Until last year, the combination of pegylated-interferon (PEG-IFN) with ribavirin (RBV) was the standard therapy, resulting in a sustained virologic response (SVR) in about half of the patients receiving this treatment [4]. Two inhibitors of HCV NS3-4A protease, telaprevir and boceprevir, were recently approved as the first directly acting antiviral reagents for the treatment of HCV genotype 1, and have been used in combination with PEG-IFN and RBV [5]. The SVR rate in the treatment of HCV genotype 1 using the new triple therapy is expected to be more than 70% [6,7]. However, several severe side effects have appeared, such as skin rash by telaprevir, ageusia by boceprevir, and advanced anemia by telaprevir/boceprevir [6,7]. Furthermore, the rapid emergence of resistant viruses by treatment with telaprevir or boceprevir is also a serious problem [8,9], since it is expected that these resistant viruses will exhibit a resistant phenotype against other NS3-4A inhibitors developed in the future [10]. Therefore, a new type of anti-HCV reagent without severe side effects or emergence of resistant virus is still needed [10], although several anti-HCV candidates, such as NS5A and NS5B inhibitors, are currently in phase II–III development [11].

To date, human hepatoma cell line HuH-7-derived cells are used as the only the preferred culture system for robust HCV replication, and most studies on anti-HCV reagents are currently

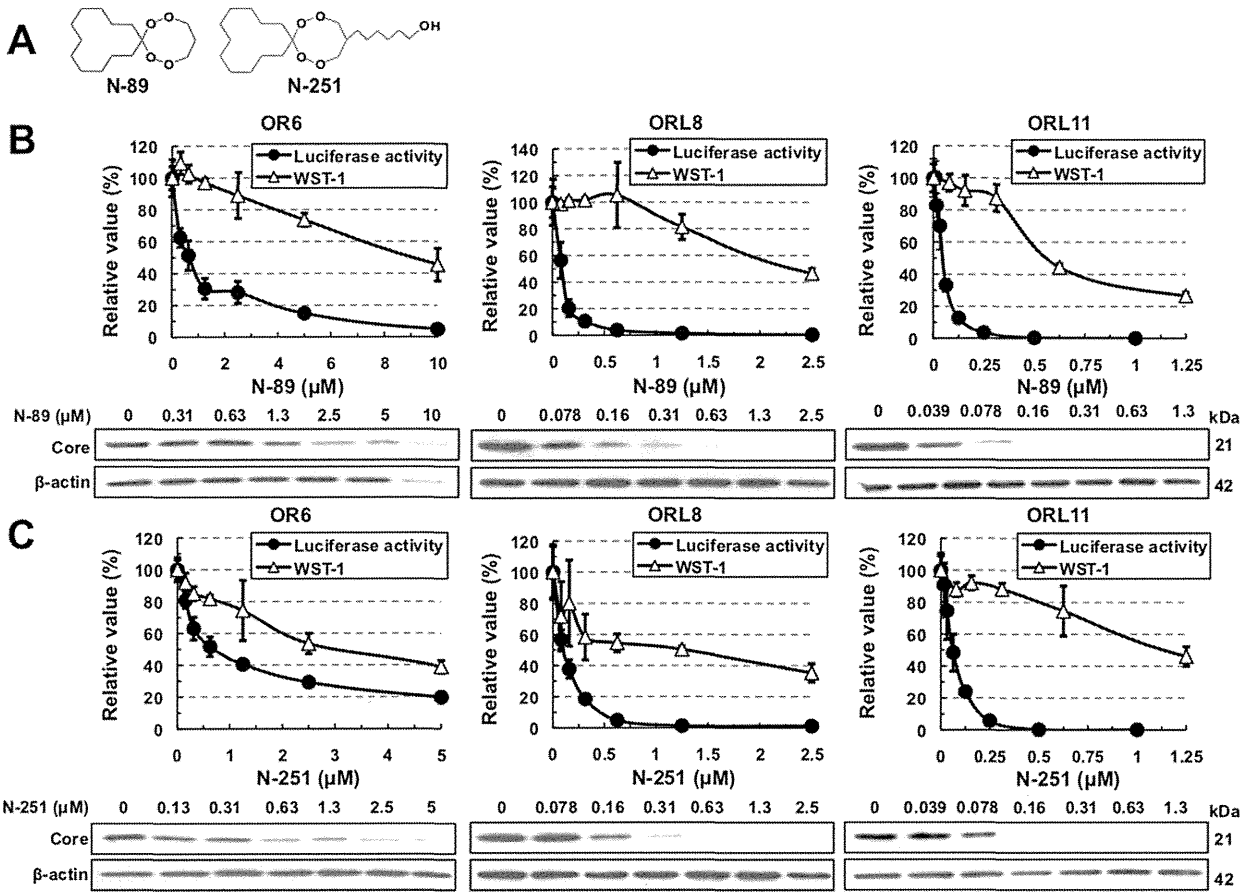

Figure 1. Anti-HCV activities of N-89 and N-251 detected in the OR6, ORL8, and ORL11 assays. (A) Structures of N-89 and N-251. (B) Effects of N-89 on genome-length HCV-RNA replication. OR6, ORL8, and ORL11 cells were treated with N-89 for 72 hrs, followed by RL assay (black circles in the upper panel) and WST-1 assay (open triangles in the upper panel). The relative value (%) calculated at each point, when the level in non-treated cells was assigned as 100%, is presented here. Data are expressed as the means±standard deviation of triplicate assays. Western blot analysis of the treated cells for the HCV Core was also performed (lower panel). β-actin was used as a control for the amount of protein loaded per lane. (C) Effects of N-251 on genome-length HCV-RNA replication. The RL assay, WST-1 assay, and Western blot analysis were performed as described in (B).
doi:10.1371/journal.pone.0072519.g001

carried out using an HuH-7-derived cell culture system [12]. We also developed an HuH-7-derived drug assay system (OR6), in which genome-length HCV-RNA (O strain of genotype 1b derived from an HCV-positive healthy carrier) encoding renilla luciferase (RL) efficiently replicates [13]. Such reporter assay systems could save time and facilitate the mass screening of anti-HCV reagents, since the values of luciferase correlated well with the level of HCV RNA after treatment with anti-HCV reagents [13]. Furthermore, OR6 assay system became more useful as a drug assay system [14] than the HCV subgenomic replicon-based reporter assay systems developed to date [12,15], because the older systems lack the core-NS2 regions containing structural proteins likely to be involved in the events that take place in the HCV-infected human liver. Indeed, by the screening of preexisting drugs using the OR6 assay system, we have identified mizoribine [16], statins [17], hydroxyurea [18], and teprenone [19] as new anti-HCV drug candidates, indicating that the OR6 assay system is useful for the discovery of anti-HCV reagents.

On the other hand, we recently found a new human hepatoma cell line, Li23, that enables efficient HCV-RNA replication and persistent HCV production, and we developed Li23-derived assay systems (ORL8 and ORL11) [20] that are comparable to the OR6 assay system [13]. Since we indicated that the gene expression profile of Li23 cells was distinct from that of HuH-7 cells [21], we expected that anti-HCV targets in Li23-derived cells might be distinct from those in HuH-7-derived cells. Indeed, we recently found that 10 μM (a clinically achievable concentration) of RBV efficiently inhibited HCV-RNA replication in the ORL8/ORL11 assays, but not in the OR6 assay [22]. This finding led us to clarify the anti-HCV mechanism of RBV [22,23]. Furthermore, we demonstrated that plural assay systems including OR6 and ORL8 were required for the objective evaluation of anti-HCV reagents [24]. In that study, we observed that the antimalarial drug artemisinin possessed weak anti-HCV activity, as reported previously [25].

From these results, we considered that antimalarial drugs might be good candidates for anti-HCV reagents, since the proliferation of both HCV and malaria generally occurs in hepatocytes. We therefore examined the anti-HCV activity of two preclinical antimalarial drugs, N-89 and its derivative water soluble N-251, which were previously discovered by our group as promising antimalarial reagents [26–28]. Here we report that N-89 and N-251 exhibit very fast and potent anti-HCV activities and have promise as potential anti-HCV drugs.

Table 1. Anti-HCV activities of N-89 or N-251 in various HCV drug assay systems.

Cell origin	HuH-7						Li23							
HCV strain	**O**		**1B-4**		**AH1**		**O**		**O**		**1B-4**		**KAH5**	
Assay	OR6		1B-4R		AH1R		ORL8		ORL11		1B-4RL		KAH5RL	
Reagents	9.0[*1]	14[*3]	9.3	22	>0.5	>20	2.3	26	0.56	12	2.4	20	2.5	13
N-89	0.66[*2]		0.42		0.025		0.089		0.045		0.12		0.19	
N-251	3.0	4.4	3.8	3.9	0.49	3.5	1.3	13	1.1	19	1.9	8.3	2.8	10
	0.69		0.98		0.14		0.10		0.059		0.23		0.29	
HCV strain	O						O		O					
Assay	sOR						sORL8		sORL11					
Reagents	1.7	2.9					1.1	9.2	1.7	14				
N-89	0.58						0.12		0.12					
N-251	2.2	3.2					4.1	19	3.1	11				
	0.69						0.22		0.27					

[*1] CC_{50} value (μM),
[*2] EC_{50} value (μM),
[*3] SI value.
doi:10.1371/journal.pone.0072519.t001

Materials and Methods

Cell Culture

RSc and D7 cells were derived from the cell lines HuH-7 and Li23, respectively, were cultured as described previously [20,29]. HuH-7-derived OR6 [13], AH1R [30], and 1B-4R [Ikeda et al., submitted] cells harboring genome-length HCV-RNA and HuH-7-derived polyclonal sOR [31], and RSc-JRN/35B [Ikeda et al., submitted] cells harboring an HCV subgenomic replicon were cultured with medium in the presence of G418 (0.3 mg/ml; Geneticin, Invitrogen, Carlsbad, CA) as described previously [13]. Li23-derived ORL8 [20], ORL11 [20], 1B-4RL [Ikeda et al., submitted], and KAH5RL [Ikeda et al., submitted] cells harboring genome-length HCV-RNA were maintained with medium in the presence of G418 (0.3 mg/ml) as described previously [20]. Li23-derived polyclonal sORL8 and sORL11 cells harboring an HCV replicon, which were established by the transfection of ORN/3-5B/QR,KE,SR RNA into the cured OL8 and OL11 cells, respectively, were also cultured with medium in the presence of G418 (0.3 mg/ml) as described previously [20]. Cured cells, from which the HCV-RNA had been eliminated by IFN treatment, were also maintained with medium in the absence of G418 as described previously [13]. HCV-RNA-replicating cells possess the G418-resistant phenotype because neomycin phosphotransferase as a selective marker was produced by the efficient replication of HCV-RNA. Therefore, when HCV-RNA is excluded from the cells or when its level is decreased, the cells are killed in the presence of G418.

Reagents

N-89 and N-251 were synthesized according to the methods described previously [26–28]. RBV was kindly provided by Yamasa (Chiba, Japan). Human IFN-α and vitamin E (VE) were purchased from Sigma-Aldrich (St. Louis, MO). Cyclosporine A (CsA) was purchased from Tokyo Chemical Industry (Tokyo, Japan). Artemisinin was purchased from Alexis Biochemicals (San Diego, CA).

RL Assay

RL assay was performed as described previously [20,24]. Briefly, the cells were plated onto 24-well plates (2×10^4 cells per well) in triplicate and then treated with each reagent at several concentrations for 72 hrs. After treatment, the cells were subjected to luciferase assay using the RL assay system (Promega, Madison, WI). The experiments were performed at least in triplicate. From the assay results, the 50% effective concentration (EC_{50}) of each reagent was determined.

WST-1 Cell Proliferation Assay

The WST-1 cell proliferation assay was performed as described previously [24]. Briefly, The cells were plated onto 96-well plates (1×10^3 cells per well) in triplicate and then treated with each reagent at several concentrations for 72 hrs. After treatment, the cells were subjected to the WST-1 cell proliferation assay (Takara Bio, Otsu, Japan) according to the manufacturer's protocol. This assay is based on the enzymatic cleavage of the tetrazolium salt WST-1 to formazan by cellular mitochondrial dehydrogenases present in viable cells. Therefore, there are viable cells even if the value of the WST-1 assay becomes zero. The experiments were performed at least in triplicate. From the assay results, the 50% cytotoxic concentration (CC_{50}) of each reagent was determined.

Western Blot Analysis

The preparation of cell lysates, sodium dodecyl sulfate-polyacrylamide gel electrophoresis, and immunoblotting analysis were performed as previously described [32]. The antibodies used in this study were those against HCV Core (CP11; Institute of Immunology, Tokyo, Japan), NS5B (a generous gift from Dr. M. Kohara, Tokyo Metropolitan Institute of Medical Science), and β-actin (AC-15; Sigma-Aldrich) as the control for the amount of protein loaded per lane.

Selective Index (SI)

The SI value of each reagent was determined by dividing the CC_{50} value by the EC_{50} value.

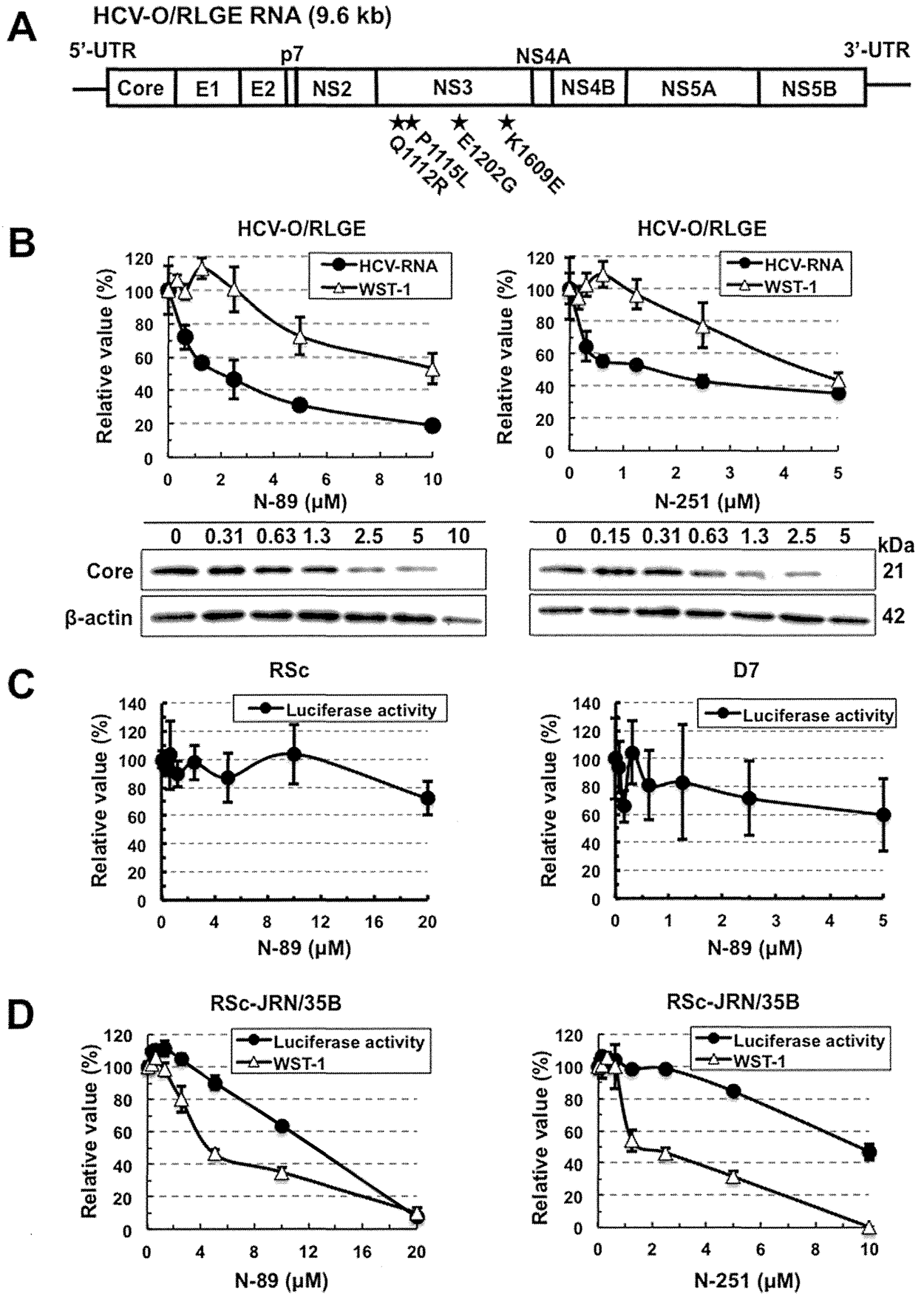
A
HCV-O/RLGE RNA (9.6 kb)
5'-UTR
p7
NS4A
3'-UTR
Core
E1
E2
NS2
NS3
NS4B
NS5A
NS5B
P1115L
Q1112R
E1202G
K1609E
B
HCV-O/RLGE
HCV-RNA
WST-1
Relative value (%)
N-89 (μM)
HCV-O/RLGE
HCV-RNA
WST-1
Relative value (%)
N-251 (μM)
0 0.31 0.63 1.3 2.5 5 10
0 0.15 0.31 0.63 1.3 2.5 5
kDa
Core
21
β-actin
42
C
RSc
Luciferase activity
Relative value (%)
N-89 (μM)
D7
Luciferase activity
Relative value (%)
N-89 (μM)
D
RSc-JRN/35B
Luciferase activity
WST-1
Relative value (%)
N-89 (μM)
RSc-JRN/35B
Luciferase activity
WST-1
Relative value (%)
N-251 (μM)

Figure 2. Characterization of anti-HCV activities of N-89 and N-251. (A) Schematic gene organization of authentic HCV-RNA (HCV-O/RLGE). The positions of four adaptive mutations - Q1112R, P1115L, E1202G, and K1609E - are indicated by a black star. (B) N-89 and N-251 inhibited authentic HCV-RNA replication. The cells harboring HCV-O/RLGE RNA [19] were treated with N-89 (left panel) and N-251 (right panel) for 72 hrs, followed by real-time LightCycler PCR (black circles in the upper panel) and WST-1 assay (open triangles in the upper panel). The relative value (%) calculated at each point, when the level in non-treated cells was assigned as 100%, is presented here. Data are expressed as the means±standard deviation of triplicate assays. Western blot analysis (lower panels) was performed as described in Fig. 1B. (C) N-89 did not inhibit the HCV-JFH-1 replication. RSc (left panel) and D7 (right panel) cells were inoculated with supernatant from RSc cells replicating JR/C5B/BX-2 [29]. The RL assay was performed as described in Fig. 1B. (D) N-89 (left panel) and N-251 (right panel) did not inhibit the replication of HCV-JFH-1 subgenomic replicon. The RL and WST-1 assays were performed as described in Fig. 1B.
doi:10.1371/journal.pone.0072519.g002

Quantitative RT-PCR Analysis

The RNAs from HCV-RNA replicating cell lines were prepared with an RNeasy extraction kit (Qiagen). The quantitative RT-PCR analysis for HCV-RNA was performed using a real-time LightCycler PCR (Roche Diagnostics, Basel, Switzerland) as described previously [13,20].

HCV Infection

HCV infection was performed as described previously [29]. RSc and D7 cells were inoculated with supernatant from RSc cells replicating JR/C5B/BX-2 [29].

Statistical Analysis

Determination of the significance of differences among groups was assessed using the Student's *t*-test. $P<0.05$ was considered significant.

Results

Preclinical Antimalarial Drugs, N-89 and N-251, Showed Potent Anti-HCV Activities in Both HuH-7- and Li23-derived Genome-length HCV-RNA-replicating Cells

Recently we demonstrated that plural HCV assay systems developed using both HuH-7 and Li23 cell lines or HCV strains belonging to genotype 1b are required for the objective evaluation of anti-HCV candidates [24]. In the present work, we used our previously developed HCV assay systems to evaluate preclinical antimalarial drugs (N-89 and N-251). N-89 (1,2,6,7-Tetraoxaspiro[7.11]nonadecane) is a chemically synthesized endoperoxide compound (Fig. 1A) with potent antimalarial activity against *Plasmodium falciparum in vitro* and *Plasmodium berghei in vivo*, and it shows low levels of cytotoxicity in mice and rats (50% lethal dose: >2000 mg/kg) [26,33,34]. N-251 (6-(1,2,6,7-tetraoxaspiro[7.11]-nonadec-4-yl)hexan-1-ol), which bears a functional side chain hydroxyl group that allows derivatization, is synthesized by replacing the hydrogen at C-4 of N-89 with hexanol (Fig. 1A), and it is as potent as N-89 against malaria parasites [27,28]. We first evaluated the anti-HCV activities of N-89 and N-251 using HuH-7-derived OR6 and Li23-derived ORL8 and ORL11 assay systems. The results revealed that both N-89 and N-251 possessed strong anti-HCV activities (Fig. 1B and C). The EC_{50} and SI values of N-89 in each assay were calculated (EC_{50} 0.66 μM, SI 14 in OR6 assay; EC_{50} 0.089 μM, SI 26 in ORL8 assay; EC_{50} 0.045 μM, SI 12 in ORL11 assay) (Table 1), and the anti-HCV activity of N-251 was found to be as potent as that of N-89 (Table 1). The anti-HCV activities of N-89 and N-251 were confirmed by Western blot analysis of HCV Core (Fig. 1B and C). To further evaluate the activities of N-89 and N-251, as additional assay systems, we used HuH-7-derived 1B-4R (1B-4 strain [31] of

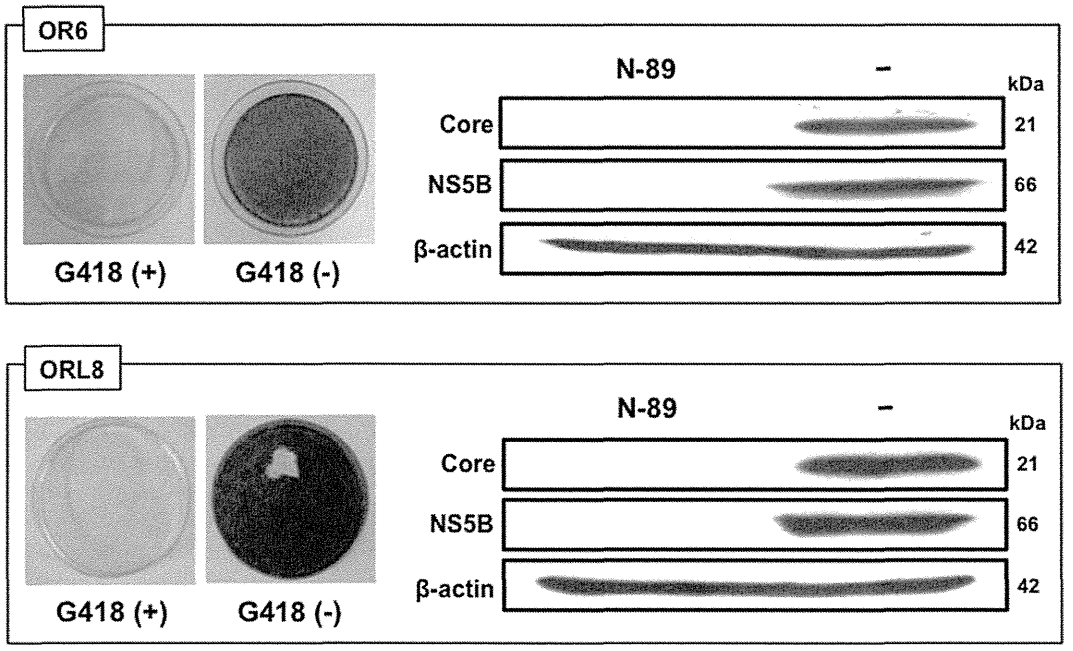

Figure 3. OR6 and ORL8 cells were cured by treatment with only N-89. The treated cells were divided into two plates with or without G418, and then cultured for 2 weeks. The left panels show the cells stained with Coomassie brilliant blue. The right panels show the results of Western blot analysis of the treated and non-treated cells for HCV proteins. Western blot analysis was performed as described in Fig. 1B.
doi:10.1371/journal.pone.0072519.g003

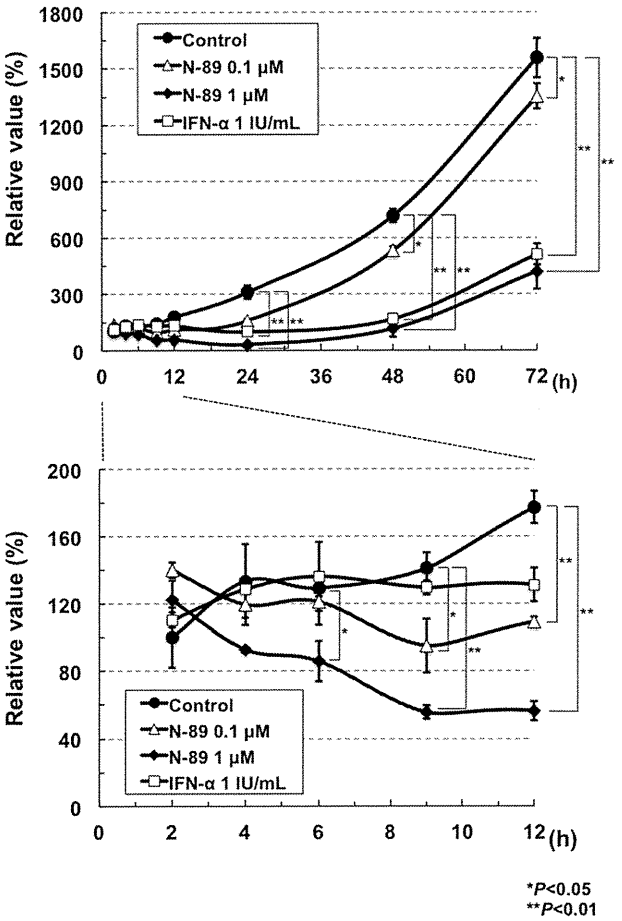

Figure 4. The anti-HCV action of N-89 was faster than that of IFN-α. The ORL8 cells were treated with N-89 or IFN-α, and then RL assays were performed at 2 to 72 hrs after the treatment. The relative value (%) calculated at each time point, when the luciferase activity of non-treated cells at 24 hrs was assigned as 100%, is shown. Data are expressed as the means±standard deviation of triplicate assays. The data within 12 hrs after the treatment are shown in the lower panel. *$P<0.05$; **$P<0.01$.**The** Anti-**HCV** Activities **of N-89 and N-251 were** Completely Canceled **by VE**We previously reported that the antioxidant VE canceled the anti-HCV activities of CsA and three nutrients (β-carotene, vitamin D_2, and linoleic acid) [37], and demonstrated that the oxidative stress induced by these anti-HCV reagents caused anti-HCV status via activation of the extracellular signal-regulated kinase signaling pathway [38]. To evaluate this possibility, we examined the effect of VE on N-89 at the EC_{90} level in the ORL8 assay. CsA and IFN-α were also used as a positive and a negative control, respectively, on the effect of VE in the ORL8 assay. The results revealed that the anti-HCV activities of N-89 and CsA were largely canceled by VE, whereas the activity of IFN-α was not canceled (Fig. 5A). We normalized these results by dividing the RL value obtained in the presence of VE by that in the absence of VE as described previously [22,37]. The values of N-89 and CsA were 16 and 34, respectively, whereas the value (3.2) of IFN-α was almost the same as that (3.0) of the control (Fig. 5B). Similar results were obtained by using N-251 (Fig. 5C and D). The values of N-251, CsA, and IFN-α were 13, 19, and 4.3, respectively, in comparison with the value (2.3) of the control (Fig. 5D). These results suggest that the induction of oxidative stress is associated with the anti-HCV activity of N-89 or N-251. However, an antimalarial drug, artemisinin, was hardly influenced by co-treatment with VE (Fig. 5E). The value (1.9) of artemisinin was almost the same as that (3.5 or 2.5) of IFN-α or the control, respectively (Fig. 5F). These results were also confirmed by Western blot analysis of HCV Core (Fig. 5G). Therefore, our results suggest that the anti-HCV mechanism of artemisinin is not associated with the induction of oxidative stress, and is distinct from that of N-89 or N-251.

doi:10.1371/journal.pone.0072519.g004

genotype 1b derived from an HCV-positive healthy carrier) [Ikeda et al., submitted] and AH1R (an AH1 strain [35] of genotype 1b derived from a patient with acute hepatitis C) [30], and Li23-derived 1B-4RL (1B-4 strain [31]) and KAH5RL (KAH5 strain [31] of genotype 1b derived from a patient with acute hepatitis C) [Ikeda et al., submitted]. These assays also showed that N-89 and N-251 possessed potent anti-HCV activities (Fig. S1A–D and Table 1). It was noteworthy that N-89 exhibited the strongest anti-HCV activity (EC_{50} 0.025 μM; SI >20) in the AH1R assay (Fig. S1A and Table 1). These results suggest that the anti-HCV activity of N-89 or N-251 is not influenced by the cell line or HCV strain. We next examined the activities of N-89 and N-251 using polyclonal cell-based assay systems (HuH-7-derived sOR [31], Li23-derived sORL8 and sORL11 [22]) that facilitate the monitoring replication of HCV subgenomic replicon RNA. These assays also showed that N-89 and N-251 possessed anti-HCV activity with EC_{50} values of less than 1 μM (Fig. S1E-G and Table 1). Taken together, these results indicate that the anti-HCV activities of N-89 and N-251 are not dependent on the specific cloned cell line or HCV structural proteins.

N-89 and N-251 Inhibited Authentic HCV-RNA Replication

The genome-length HCV-RNA used in the assay systems described above contains three non-natural elements: RL, neomycin phosphotransferase, and an internal ribosomal entry site of encephalomyocarditis virus. To exclude the possibility that the anti-HCV activity of N-89 or N-251 was due to the inhibition of these three exogenous elements, we examined the anti-HCV activities of N-89 and N-251 using the authentic 9.6 kb HCV-RNA-replicating HCV-O/RLGE cells [19], which were developed by the introduction of *in vitro* synthesized HCV-O/RLGE RNA (Fig. 2A) into OR6c cured cells. We could demonstrate by quantitative RT-PCR and Western blot analyses that N-89 and N-251 at the expected concentrations efficiently prevented HCV-RNA replication and HCV Core expression in HCV-O/RLGE cells in a dose-dependent manner, respectively (Fig. 2B). The EC_{50} and SI values of N-89 and N-251 in this assay were calculated as follows each: EC_{50} 2.0 μM and SI >5.0 in N-89; EC_{50} 1.6 μM and SI 2.8 in N-251. To further confirm that N-89 or N-251 does not inhibit the RL activity, we examined the direct effect of each reagent by adding it along with substrate to the cell lysate in the RL assay. No suppressive effects by N-89 and N-251 were observed in either the OR6 assay (Fig. S2A) or the ORL8 assay (Fig. S2B). These results indicate that the anti-HCV activities of N-89 and N-251 were due to the inhibition of HCV-RNA itself, but not to exogenous elements contained in the genome-length HCV-RNA.

N-89 and N-251 did not Inhibit RNA Replication of HCV-JFH-1 Strain

We next examined whether N-89 and N-251 worked in an HCV production system using HCV-JFH-1 strain (genotype 2a). Unexpectedly, the results using the JFH-1 reporter assay systems [29], which were recently developed using HuH-7-derived RSc and Li23-derived D7 cells, revealed that both N-89 and N-251 did not show anti-HCV activity for the HCV-JFH-1 strain (Fig. 2C, Fig. S3). To clarify whether anti-HCV activity depends on the difference of genotype or assay model, we evaluated the activities of N-89 and N-251 using RSc-JRN/35B [Ikeda et al., submitted] cells harboring a subgenomic HCV-JFH-1 replicon as an additional assay. The results revealed that N-89 and N-251 did not show any anti-HCV activities in this assay system either (Fig. 2D). Although the relative value of WST-1 almost became zero when RSc-JRN/35B cells were treated with 10 μM of N-251,

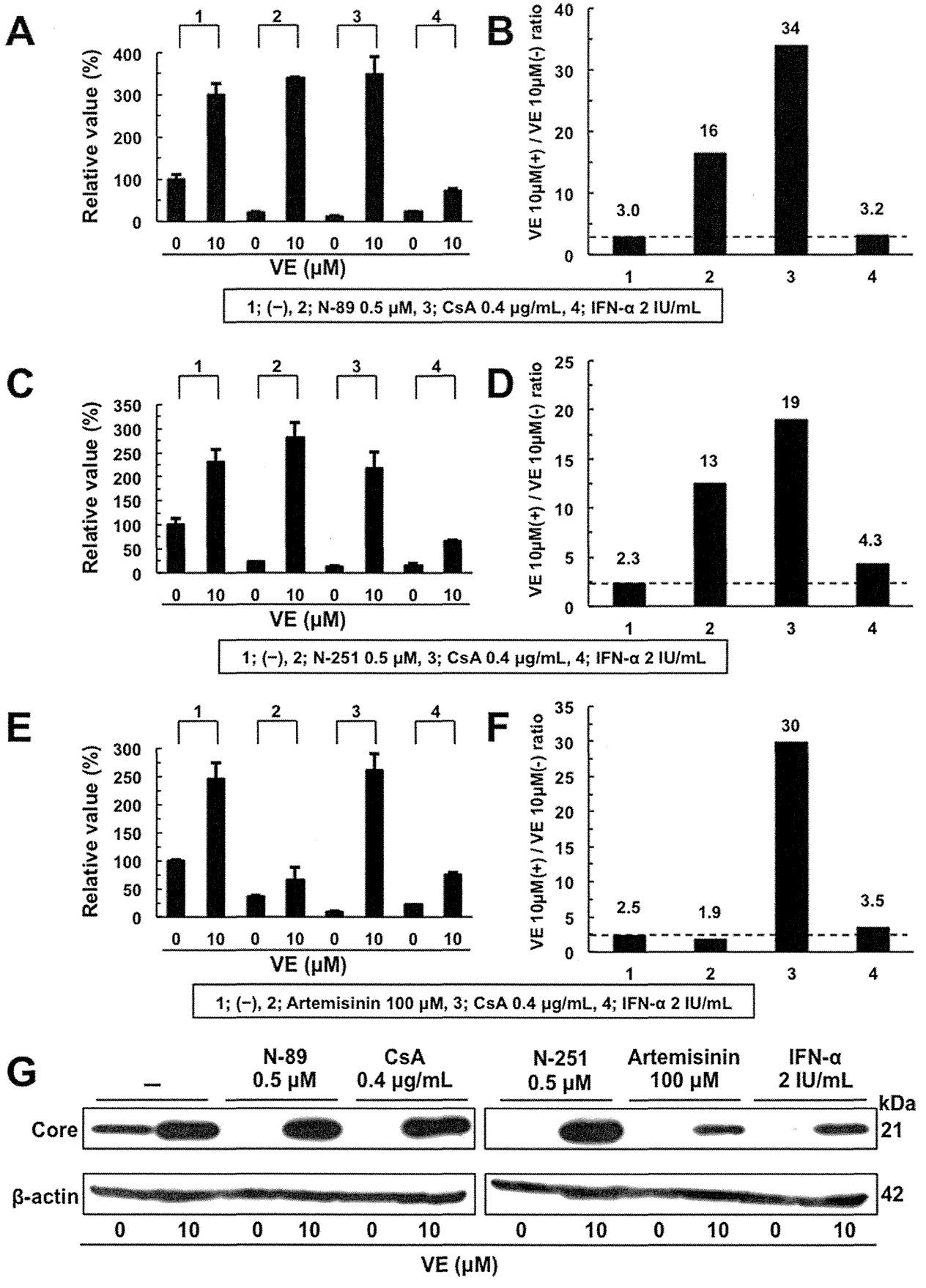
A
Relative value (%)
VE (μM)
1; (−), 2; N-89 0.5 μM, 3; CsA 0.4 μg/mL, 4; IFN-α 2 IU/mL
B
VE 10μM(+) / VE 10μM(-) ratio
3.0
16
34
3.2
C
Relative value (%)
VE (μM)
1; (−), 2; N-251 0.5 μM, 3; CsA 0.4 μg/mL, 4; IFN-α 2 IU/mL
D
VE 10μM(+) / VE 10μM(-) ratio
2.3
13
19
4.3
E
Relative value (%)
VE (μM)
1; (−), 2; Artemisinin 100 μM, 3; CsA 0.4 μg/mL, 4; IFN-α 2 IU/mL
F
VE 10μM(+) / VE 10μM(-) ratio
2.5
1.9
30
3.5
G
—
N-89 0.5 μM
CsA 0.4 μg/mL
N-251 0.5 μM
Artemisinin 100 μM
IFN-α 2 IU/mL
kDa
Core
21
β-actin
42
VE (μM)

Figure 5. The anti-HCV activity of N-89 or N-251 was canceled by addition of VE. Effect of VE on the anti-HCV activity of N-89 (A), N-251 (C), Artemisinin (E), CsA, or IFN-α at the expected EC_{90}. ORL8 cells were treated with control medium (−), N-89, CsA, or IFN-α in either the absence or presence of VE for 72 hrs. After treatment, an RL assay of harvested ORL8 cell samples was performed. (B, D, and F) The ratio of RL activity in the presence of VE to the RL activity in the absence of VE. The above ratio was calculated from the data of (A, C, and E). The horizontal line indicates the promoting effect of VE alone on HCV-RNA replication as a baseline. (G) Western blot analysis was performed as described in Fig. 1B.
doi:10.1371/journal.pone.0072519.g005

cell counting after trypan blue dye treatment revealed that approximately 30% of the cells were viable (data not shown). These results suggest that the inhibitory effect of N-89 or N-251 on HCV-RNA replication may depend on genotype 1b or not work for only JFH-1 strain.

OR6 and ORL8 Cells were Cured by Treatment with only N-89

To date, IFN-α alone or IFN-γ alone has generally been used to prepare cured cells from the cells harboring HCV-RNA [36]. Since we observed strong anti-HCV activity (>99% suppression) at 8 μM of N-89 in OR6 cells or 1 μM of N-89 in ORL8 cells without a decrease in cell viability (Fig. 1B), we expected that these cells might be cured only by treatment with N-89. Accordingly, OR6 and ORL8 cells were treated with 8 μM and 1 μM of N-89, respectively, in the absence of G418. The treatment was continued for 3 weeks with the addition of N-89 at 4-day intervals. All of the treated cells were dead when cultured in the presence of G418 for an additional two weeks, whereas the treated cells proliferated efficiently in the absence of G418 (Fig. 3), suggesting that OR6 and ORL8 cells are cured by monotherapy with N-89. This suggestion was confirmed by Western blot analysis (Fig. 3). These results indicate that N-89 is a strong anti-HCV reagent, which can be used to prepare cured cells by treatment at low concentration.

Comparative Time Course Assay of the Anti-HCV Activities of N-89 and IFN-α

We next performed a time course assay (2 to 72 hrs after treatment) in the case of ORL8 cells treated with N-89 (0.1 μM or 1 μM) or IFN-α (1 IU/ml; corresponding to approximately EC_{80}). ORL8 cells treated with IFN-α (1 IU/ml) and N-89 (1 μM) had almost the same anti-HCV kinetics over the first 24 hrs after treatment (upper panel of Fig. 4); however, within the first 12 hrs after treatment N-89-treated ORL8 cells had more rapid anti-HCV kinetics than did the IFN-α-treated cells (lower panel of Fig. 4). N-89 at concentrations of 0.1 μM and 1 μM led to

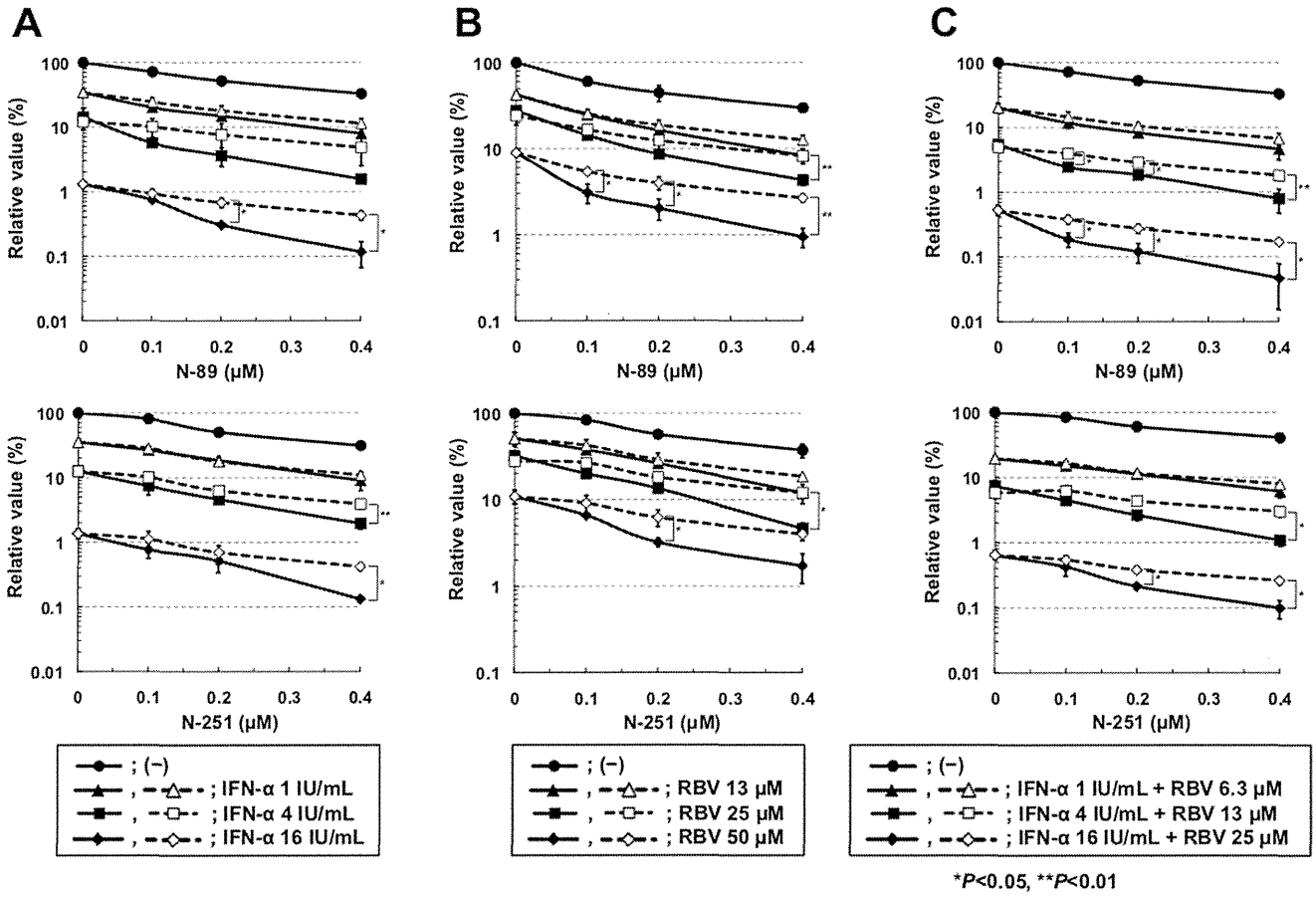

Figure 6. Synergistic anti-HCV effects of N-89 or N-251 in combination with IFN-α and/or RBV on HCV-RNA replication in ORL8 cells. Open symbols in the broken lines show the values expected as an additive anti-HCV effect and closed symbols in the solid lines show the values obtained by the ORL8 assay. ORL8 cells were treated with N-89 (upper panel) or N-251 (lower panel) in combination with IFN-α (A), RBV (B), or IFN-α and RBV (C) for 72 hrs and subjected to RL assay.
doi:10.1371/journal.pone.0072519.g006

significantly decreased RL activity at 9 hrs and 6 hrs, respectively, after treatment, whereas a decrease of RL activity in the cells treated with 1 IU/ml of IFN-α began to be seen at 12 hrs after treatment (lower panel of Fig. 4). These results suggest that the action of N-89, and probably also that of N-251, is faster than that of IFN-α, and the anti-HCV mechanism of N-89 is different from that of IFN-α.

Synergistic Effect of Anti-HCV Activity by N-89 or N-251 in Combination with IFN-α and/or RBV

We examined the anti-HCV activity of N-89 or N-251 in combination with IFN-α using OR6 and ORL8 assay systems. The results of the ORL8 assay revealed that the anti-HCV activity of N-89 or N-251 in combination with IFN-α (more than 4 IU/ml) was significantly stronger than that expected as an additive effect, suggesting a synergistic effect of N-89 or N-251 and IFN-α (Fig. 6A). However, such an effect was not clear in the OR6 assay (Fig. S4A). We recently demonstrated that 10 μM (a clinically achievable concentration) of RBV efficiently inhibited HCV-RNA replication in the ORL8 assay [22], and demonstrated that adenosine kinase, which phosphorylates RBV to generate monophosphorylated RBV possessing the inhibitory activity for inosine monophosphate dehydrogenase, is an essential determinant of the anti-HCV activity of RBV in cell culture [23]. Therefore, we next examined the combination effect of RBV in the same way as IFN-α using an ORL8 assay. We observed that the anti-HCV activity of N-89 or N-251 in combination with RBV was significantly stronger than that expected additively, suggesting that there was a synergistic effect between N-89 or N-251 and RBV (Fig. 6B). However, in the OR6 assay, we noticed that RBV showed an additive anti-HCV effect in combination with N-89 or N-251 (Fig. S4B). Since RBV has been shown to have little anti-HCV activity in the OR6 assay system [22], some specific factor(s) in ORL8 cells might contribute to the synergistic effect of N-89 or N-251 in combination with RBV. Therefore, we further examined the effect of N89 or N-251 in combination with both IFN-α and RBV using an ORL8 assay. As expected, the anti-HCV activity of N-89 or N-251 was synergistically enhanced in combination with both IFN-α and RBV in the ORL8 assay (Fig. 6C). On the other hand, in the OR6 assay, a synergistic effect like that seen in the ORL8 assay was not observed (Fig. S4C). We confirmed that any such synergistic effect was not due to the cell toxic effect (Fig. S5).

Discussion

N-89 and its derivative N-251 are preclinical and promising drugs possessing antimalarial activities *in vitro* and *in vivo* comparable to those of artemisinin [26,27]. In the present study, using cell-based HCV-RNA-replication assay systems, we found that N-89 and N-251 possessed potent anti-HCV activities irrespective of the cell lines and HCV strains of genotype 1b, and that they did not work for JFH-1 strain of genotype 2a. Furthermore, We demonstrated that the anti-HCV kinetics of N-89 was faster than that of IFN-α, and that both N-89 and N-251 exhibited synergistic effects in combination with IFN-α and/or RBV.

Along with the worldwide spread of HCV, high prevalence areas of HCV infection have overlapped with endemic areas of malaria infection [39,40]. It is also interesting that the liver is a target organ for the replication of HCV and malaria. This fact would again suggest that N-89 and N-251 target a common factor that is required for the replication of HCV and malaria. At the same time, N-89 and N-251 have become readily and cheaply available due to their ease of synthesis [26,27]. Since we showed that HCV-RNA-replicating cells were cured by monotherapy with N-89, monotherapy with N-89 or N-251 would be simultaneously effective for the diseases caused by malaria and HCV infection. Furthermore, we recently showed that the blood concentration of N-89 or N-251 reaches approximately 1 μM [Kim et al., unpublished data]. Since this concentration, which is equivalent to the EC_{99} value of N-89 in the ORL8 assay, was used for the preparation of cured cells, even monotherapy with N-89 would be useful for patients with chronic hepatitis C.

In regard to the anti-HCV mechanism of N-89 and N-251, we provided evidence that the anti-HCV activity of these reagents was canceled by antioxidant VE, suggesting the induction of oxidative stress. To identify the target factor(s) located downstream of ROS production, we attempted microarray analysis using OR6 and ORL8 cells treated with N-89. However, consequently, we failed to obtain the candidate gene indicating the meaningful expression level, although we identified several genes, which were commonly upregulated or downregulated in the N-89-treated cells (Fig. S6). On the other hand, it has been recently reported that *Plasmodium falciparum* endoplasmic reticulum-resident calcium binding protein is a possible target of N-89 and N-251 [41]. Therefore, this protein may be involved in the anti-HCV activities of N-89 and N-251. To clarify the factor(s), further analysis will be needed.

The synergistic anti-HCV effect of N-89 or N-251 in combination with RBV rather than IFN-α is also interesting. Using RBV-sensitive ORL8 cells, we recently clarified that the anti-HCV mechanism of RBV was mediated by the inhibition of IMPDH, which is required for HCV-RNA replication [22]. In addition, since RBV is an important component of current IFN-based therapies, including the recently developed triple therapy, the use of N-89 or N-251 may further enhance the SVR rate achieved with the current therapy. Furthermore, recent report [42] that the *lead-in* four weeks of RBV treatment before starting a standard course of PEG-IFN with RBV led a weak decrease of viral replication (0.5 ± 0.5 $\log_{10}$) is noteworthy. To evaluate this possibility, we compared the SI values of N-89, N-251, RBV, and CsA using the ORL8 assay system. The results revealed that the SI values of N-89, N-251, RBV, and CsA were 26, 13, 10, and 15, respectively, indicating that the anti-HCV activity of N-89 or N-251 is equivalent to that of RBV or CsA. Since the treatment with N-89/N-251 and RBV exhibits a synergistic effect, oral N-89 or N-251 would be good compounds for inclusion in the current triple therapy.

In conclusion, we found that two oral antimalarial drugs in the preclinical stage of development (N-89 and N-251) exhibited strong anti-HCV activities to genotype 1b. These compounds would have potential as one component of a therapeutic regimen based on combinations of HCV-specific inhibitors.

Supporting Information

Figure S1 Anti-HCV activities of N-89 and N-251 detected in the several assay systems using genome-length HCV-RNA or HCV subgenomic replicon RNA. (A) Effects of N-89 and N-251 on genome-length HCV-RNA (AH1 strain of genotype 1b) replication in the AH1R assay. AH1R cells were treated with N-89 or N-251 for 72 hrs, followed by RL assay (black circles) and WST-1 assay (open triangles). The relative value (%) calculated at each point, when the level in non-treated cells was assigned as 100%, is presented here. Data are expressed as the means ± standard deviation of triplicate assays. (B) Effects of N-89 and N-251 on genome-length HCV-RNA (HCV 1B-4 strain of genotype 1b) replication in the 1B-4R assay. The RL assay and WST-1 assay were performed as described in (A). (C) Effects of N-89 and N-251 on genome-length HCV-RNA (HCV 1B-4 strain of

genotype 1b) replication in the 1B-4RL assay. The RL assay and WST-1 assay were performed as described in (A). (D) Effects of N-89 and N-251 on genome-length HCV-RNA (HCV KAH5 strain of genotype 1b) replication in the KAH5RL assay. The RL assay and WST-1 assay were performed as described in (A). (E) Effects of N-89 and N-251 on HCV subgenomic replicon RNA (HCV O strain of genotype) replication in the sOR assay. The RL assay and WST-1 assay were performed as described in (A). (F) Effects of N-89 and N-251 on HCV subgenomic replicon RNA (HCV O strain of genotype 1b) replication in the sORL8 assay. The RL assay and WST-1 assay were performed as described in (A). (G) Effects of N-89 and N-251 on HCV subgenomic replicon RNA (HCV O strain of genotype 1b) replication in the sORL11 assay. The RL assay and WST-1 assay were performed as described in (A).
(TIF)

Figure S2 No inhibition of RL activity by N-89 or N-251. (A) N-89 and N-251 did not inhibit the RL activity in the OR6 cell lysate. N-89 or N-251 was added to the OR6 cell lysate, and then an RL assay was performed. (B) N-89 and N-251 did not inhibit the RL activity in the ORL8 cell lysate. N-89 or N-251 was added to the ORL8 cell lysate, and then an RL assay was performed.
(TIF)

Figure S3 N-251 did not inhibit the HCV-JFH-1 replication. RSc and D7 cells were inoculated with supernatant from RSc cells replicating JR/C5B/BX-2 [2]. The RL assay was performed as described in Fig. S1A.
(TIF)

Figure S4 Anti-HCV effects of N-89 or N-251 in combination with IFN-α and/or RBV on HCV-RNA replication in OR6 cells. Open symbols in the broken lines show the values expected as an additive anti-HCV effect and closed symbols in the solid lines show the values obtained by the OR6 assay. (A) Effect of N-89 or N-251 in combination with IFN-α on OR6 assay. OR6 cells were treated with N-89 (upper panel) or N-251 (lower panel) in combination with IFN-α for 72 hrs and subjected to RL assay. (B) Effect of N-89 or N-251 in combination with RBV on OR6 assay. OR6 cells were treated with N-89 (upper panel) or N-251 (lower panel) in combination with RBV for 72 hrs and subjected to RL assay. (C) Effect of N-89 or N-251 in combination with IFN-α and RBV on OR6 assay. OR6 cells were treated with N-89 (upper panel) or N-251 (lower panel) in combination with IFN-α and RBV for 72 hrs and subjected to RL assay.
(TIF)

Figure S5 Effects of N-89 or N-251 in combination with IFN-α and/or RBV on the growth of ORL8 or OR6 cells. ORL8 cells (A, B) or OR6 cells (C, D) were treated with N-89 (A, C) or N-251 (B, D) in combination with IFN-α for 72 hrs and subjected to the cell counting. The cell counting was carried out as described in the Supporting Materials and methods.
(TIF)

Figure S6 Selection of genes whose expression levels were commonly upregulated or downregulated in the N-89-treated OR6 and ORL8 cells. (A) Genes whose expression levels were upregulated at ratios of more than 2 in the case of OR6(−) versus OR6(N-89) or ORL8(−) versus ORL8(N-89) were selected. 4 genes upregulated commonly in the N-89-treated cells were listed. (B) Genes whose expression levels were downregulated at ratios of less than 0.5 in the case of OR6(−) versus OR6(N-89) or ORL8(−) versus ORL8(N-89) were selected. 5 genes downregulated commonly in the N-89-treated cells were listed.
(TIF)

Text S1.
(DOC)

Acknowledgments

We thank Yoshimi Kawae for her technical assistances. We also thank Dr. Hiroyuki Doi (Okayama University, Japan) for his helpful suggestions.

Author Contributions

Conceived and designed the experiments: YU NK. Performed the experiments: YU MT. Analyzed the data: YU NK. Contributed reagents/materials/analysis tools: KM HD TW HSK AS YW MI. Wrote the paper: YU NK.

References

1. Thomas DL (2000) Hepatitis C epidemiology. Curr Top Microbiol Immunol 242: 25–41.
2. Kato N (2001) Molecular virology of hepatitis C virus. Acta Med Okayama 55: 133–159.
3. Kato N, Hijikata M, Ootsuyama Y, Nakagawa M, Ohkoshi S, et al. (1990) Molecular cloning of the human hepatitis C virus genome from Japanese patients with non-A, non-B hepatitis. Proc Natl Acad Sci U S A 87: 9524–9528.
4. Chevaliez S, Pawlotsky JM (2007) Interferon-based therapy of hepatitis C. Adv Drug Deliv Rev 59: 1222–1241.
5. Ghany MG, Nelson DR, Strader DB, Thomas DL, Seeff LB (2011) An update on treatment of genotype 1 chronic hepatitis C virus infection: 2011 practice guideline by the American Association for the Study of Liver Diseases. Hepatology 54: 1433–1444.
6. Jacobson IM, McHutchison JG, Dusheiko G, Di Bisceglie AM, Reddy KR, et al. (2011) Telaprevir for previously untreated chronic hepatitis C virus infection. N Engl J Med 364: 2405–2416.
7. Poordad F, McCone J Jr, Bacon BR, Bruno S, Manns MP, et al. (2011) Boceprevir for untreated chronic HCV genotype 1 infection. N Engl J Med 364: 1195–1206.
8. Reesink HW, Zeuzem S, Weegink CJ, Forestier N, van Vliet A, et al. (2006) Rapid decline of viral RNA in hepatitis C patients treated with VX-950: a phase Ib, placebo-controlled, randomized study. Gastroenterology 131: 997–1002.
9. Susser S, Welsch C, Wang Y, Zettler M, Domingues FS, et al. (2009) Characterization of resistance to the protease inhibitor boceprevir in hepatitis C virus-infected patients. Hepatology 50: 1709–1718.
10. Rosen HR (2011) Clinical practice. Chronic hepatitis C infection. N Engl J Med 364: 2429–2438.
11. Pawlotsky JM (2011) Treatment failure and resistance with direct-acting antiviral drugs against hepatitis C virus. Hepatology 53: 1742–1751.
12. Bartenschlager R, Sparacio S (2007) Hepatitis C virus molecular clones and their replication capacity in vivo and in cell culture. Virus Res 127: 195–207.
13. Ikeda M, Abe K, Dansako H, Nakamura T, Naka K, et al. (2005) Efficient replication of a full-length hepatitis C virus genome, strain O, in cell culture, and development of a luciferase reporter system. Biochem Biophys Res Commun 329: 1350–1359.
14. Ikeda M, Kato N (2007) Modulation of host metabolism as a target of new antivirals. Adv Drug Deliv Rev 59: 1277–1289.
15. Moradpour D, Penin F, Rice CM (2007) Replication of hepatitis C virus. Nat Rev Microbiol 5: 453–463.
16. Naka K, Ikeda M, Abe K, Dansako H, Kato N (2005) Mizoribine inhibits hepatitis C virus RNA replication: effect of combination with interferon-alpha. Biochem Biophys Res Commun 330: 871–879.
17. Ikeda M, Abe K, Yamada M, Dansako H, Naka K, et al. (2006) Different anti-HCV profiles of statins and their potential for combination therapy with interferon. Hepatology 44: 117–125.
18. Nozaki A, Morimoto M, Kondo M, Oshima T, Numata K, et al. (2010) Hydroxyurea as an inhibitor of hepatitis C virus RNA replication. Arch Virol 155: 601–605.
19. Ikeda M, Kawai Y, Mori K, Yano M, Abe K, et al. (2011) Anti-ulcer agent teprenone inhibits hepatitis C virus replication: potential treatment for hepatitis C. Liver Int 31: 871–880.
20. Kato N, Mori K, Abe K, Dansako H, Kuroki M, et al. (2009) Efficient replication systems for hepatitis C virus using a new human hepatoma cell line. Virus Res 146: 41–50.
21. Mori K, Ikeda M, Ariumi Y, Kato N (2010) Gene expression profile of Li23, a new human hepatoma cell line that enables robust hepatitis C virus replication: Comparison with HuH-7 and other hepatic cell lines. Hepatol Res 40: 1248–1253.

22. Mori K, Ikeda M, Ariumi Y, Dansako H, Wakita T, et al. (2011) Mechanism of action of ribavirin in a novel hepatitis C virus replication cell system. Virus Res 157: 61–70.
23. Mori K, Hiraoka O, Ikeda M, Ariumi Y, Hiramoto A, et al. (2013) Adenosine kinase is a key determinant for the anti-HCV activity of ribavirin. Hepatology in press.
24. Ueda Y, Mori K, Ariumi Y, Ikeda M, Kato N (2011) Plural assay systems derived from different cell lines and hepatitis C virus strains are required for the objective evaluation of anti-hepatitis C virus reagents. Biochem Biophys Res Commun 409: 663–668.
25. Paeshuyse J, Coelmont L, Vliegen I, Van Hemel J, Vandenkerckhove J, et al. (2006) Hemin potentiates the anti-hepatitis C virus activity of the antimalarial drug artemisinin. Biochem Biophys Res Commun 348: 139–144.
26. Kim HS, Nagai Y, Ono K, Begum K, Wataya Y, et al. (2001) Synthesis and antimalarial activity of novel medium-sized 1,2,4,5-tetraoxacycloalkanes. J Med Chem 44: 2357–2361.
27. Sato A, Hiramoto A, Morita M, Matsumoto M, Komich Y, et al. (2011) Antimalarial activity of endoperoxide compound 6-(1,2,6,7-tetraoxaspiro[7.11]-nonadec-4-yl)hexan-1-ol. Parasitol Int 60: 270–273.
28. Sato A, Kawai S, Hiramoto A, Morita M, Tanigawa N, et al. (2011) Antimalarial activity of 6-(1,2,6,7-tetraoxaspiro[7.11]nonadec-4-yl)hexan-1-ol (N-251) and its carboxylic acid derivatives. Parasitol Int 60: 488–492.
29. Takeda M, Ikeda M, Ariumi Y, Wakita T, Kato N (2012) Development of hepatitis C virus production reporter-assay systems using two different hepatoma cell lines. J Gen Virol 93: 1422–1431.
30. Mori K, Ueda Y, Ariumi Y, Dansako H, Ikeda M, et al. (2012) Development of a drug assay system with hepatitis C virus genome derived from a patient with acute hepatitis C. Virus Genes 44: 374–381.
31. Nishimura G, Ikeda M, Mori K, Nakazawa T, Ariumi Y, et al. (2009) Replicons from genotype 1b HCV-positive sera exhibit diverse sensitivities to anti-HCV reagents. Antiviral Res 82: 42–50.
32. Kato N, Sugiyama K, Namba K, Dansako H, Nakamura T, et al. (2003) Establishment of a hepatitis C virus subgenomic replicon derived from human hepatocytes infected in vitro. Biochem Biophys Res Commun 306: 756–766.
33. Aly NS, Hiramoto A, Sanai H, Hiraoka O, Hiramoto K, et al. (2007) Proteome analysis of new antimalarial endoperoxide against Plasmodium falciparum. Parasitol Res 100: 1119–1124.
34. Kim HS, Begum K, Ogura N, Wataya Y, Nonami Y, et al. (2003) Antimalarial activity of novel 1,2,5,6-tetraoxacycloalkanes and 1,2,5-trioxacycloalkanes. J Med Chem 46: 1957–1961.
35. Mori K, Abe K, Dansako H, Ariumi Y, Ikeda M, et al. (2008) New efficient replication system with hepatitis C virus genome derived from a patient with acute hepatitis C. Biochem Biophys Res Commun 371: 104–109.
36. Abe K, Ikeda M, Dansako H, Naka K, Kato N (2007) Cell culture-adaptive NS3 mutations required for the robust replication of genome-length hepatitis C virus RNA. Virus Res 125: 88–97.
37. Yano M, Ikeda M, Abe K, Dansako H, Ohkoshi S, et al. (2007) Comprehensive analysis of the effects of ordinary nutrients on hepatitis C virus RNA replication in cell culture. Antimicrob Agents Chemother 51: 2016–2027.
38. Yano M, Ikeda M, Abe K, Kawai Y, Kuroki M, et al. (2009) Oxidative stress induces anti-hepatitis C virus status via the activation of extracellular signal-regulated kinase. Hepatology 50: 678–688.
39. Feachem RG, Phillips AA, Hwang J, Cotter C, Wielgosz B, et al. (2010) Shrinking the malaria map: progress and prospects. Lancet 376: 1566–1578.
40. Shepard CW, Finelli L, Alter MJ (2005) Global epidemiology of hepatitis C virus infection. Lancet Infect Dis 5: 558–567.
41. Morita M, Sanai H, Hiramoto A, Sato A, Hiraoka O, et al. (2012) Plasmodium falciparum endoplasmic reticulum-resident calcium binding protein is a possible target of synthetic antimalarial endoperoxides, N-89 and N-251. J Proteome Res 11: 5704–5711.
42. Rotman Y, Noureddin M, Feld JJ, Guedj J, Witthaus M, et al. (2013) Effect of ribavirin on viral kinetics and liver gene expression in chronic hepatitis C. Gut in press.

Biochemical and Biophysical Research Communications 430 (2013) 592–597

Contents lists available at SciVerse ScienceDirect

Biochemical and Biophysical Research Communications

journal homepage: www.elsevier.com/locate/ybbrc

PML tumor suppressor protein is required for HCV production

Misao Kuroki [a,b,c], Yasuo Ariumi [a,c,*], Makoto Hijikata [d], Masanori Ikeda [a], Hiromichi Dansako [a], Takaji Wakita [e], Kunitada Shimotohno [f], Nobuyuki Kato [a]

[a] Department of Tumor Virology, Okayama University Graduate School of Medicine, Dentistry, and Pharmaceutical Sciences, 2-5-1, Shikata-cho, Okayama 700-8558, Japan
[b] Research Fellow of the Japan Society for the Promotion of Science
[c] Center for AIDS Research, Kumamoto University, Kumamoto 860-0811, Japan
[d] Department of Viral Oncology, Institute for Virus Research, Kyoto University, Kyoto 606-8507, Japan
[e] Department of Virology II, National Institute of Infectious Diseases, Tokyo 162-8640, Japan
[f] Research Center for Hepatitis and Immunology, National Center for Global Health and Medicine, Ichikawa, Chiba 272-8516, Japan

ARTICLE INFO

Article history:
Received 8 November 2012
Available online 5 December 2012

Keywords:
Hepatitis C virus
PML
INI1
DDX5
Tumor suppressor
Lipid droplet

ABSTRACT

PML tumor suppressor protein, which forms discrete nuclear structures termed PML-nuclear bodies, has been associated with several cellular functions, including cell proliferation, apoptosis and antiviral defense. Recently, it was reported that the HCV core protein colocalizes with PML in PML-NBs and abrogates the PML function through interaction with PML. However, role(s) of PML in HCV life cycle is unknown. To test whether or not PML affects HCV life cycle, we examined the level of secreted HCV core and the infectivity of HCV in the culture supernatants as well as the level of HCV RNA in HuH-7-derived RSc cells, in which HCV-JFH1 can infect and efficiently replicate, stably expressing short hairpin RNA targeted to PML. In this context, the level of secreted HCV core and the infectivity in the supernatants from PML knockdown cells was remarkably reduced, whereas the level of HCV RNA in the PML knockdown cells was not significantly affected in spite of very effective knockdown of PML. In fact, we showed that PML is unrelated to HCV RNA replication using the subgenomic HCV-JFH1 replicon RNA, JRN/3-5B. Furthermore, the infectivity of HCV-like particle in the culture supernatants was significantly reduced in PML knockdown JRN/3-5B cells expressing core to NS2 coding region of HCV-JFH1 genome using the *trans*-packaging system. Finally, we also demonstrated that INI1 and DDX5, the PML-related proteins, are involved in HCV production. Taken together, these findings suggest that PML is required for HCV production.

1. Introduction

Hepatitis C virus (HCV) is the causative agent of chronic hepatitis, which progresses to liver cirrhosis and hepatocellular carcinoma. HCV is an enveloped virus with a positive single-stranded 9.6 kb RNA genome, which encodes a large polyprotein precursor of approximately 3000 amino acid residues. This polyprotein is cleaved by a combination of the host and viral proteases into at least 10 proteins in the following order: core, envelope 1 (E1), E2, p7, non-structural 2 (NS2), NS3, NS4A, NS4B, NS5A, and NS5B [1,2]. HCV core protein forms a viral capsid and is essential for infectious virion production. The core protein is targeted to lipid droplets. Recently, lipid droplets have been found to be involved in an important cytoplasmic organelle for HCV production [3].

In addition, HCV core has been reported to facilitate cellular transformation as well as development of hepatocellular carcinoma in HCV core-transgenic mice [4]. Interactions of core with tumor suppressor proteins such as p53 and DDX3 may lead to enhanced cellular proliferation [4]. Indeed, HCV core interacts with promyelocytic leukemia (PML) protein and inhibits the PML tumor suppressor pathway through interfering with the PML-mediated apoptosis-inducing function [5]. PML forms discrete nuclear structures termed PML-nuclear bodies (PML-NBs) and associates with several cellular functions, including cell proliferation, apoptosis and antiviral defense [6,7]. In acute promyelocytic leukemia (APL) patient, the PML gene is fused with the retinoic acid receptor-α (RARα) gene, thus resulting in expression of an oncogenic PML-RARα fusion protein [6,7]. Conversely, treatment of APL patient with arsenic trioxide leads to reformation of PML-NBs and results in disease remission [6,7], indicating that PML is a target of arsenic trioxide. Interestingly, we have recently demonstrated that arsenic trioxide strongly inhibited HCV infection and HCV RNA replication without cell toxicity [8]. However, the role of PML in HCV life cycle yet remains unclear. To investigate the possible involvement of PML in HCV life cycle, we examined the accumulation of HCV RNA as well as the release of HCV core into culture

* Corresponding author at: Center for AIDS Research, Kumamoto University, 2-2-1, Honjo, Kumamoto 860-0811, Japan. Fax: +81 96 373 6834.
E-mail address: ariumi@kumamoto-u.ac.jp (Y. Ariumi).

0006-291X/$ - see front matter Crown Copyright © 2012 Published by Elsevier Inc. All rights reserved.
http://dx.doi.org/10.1016/j.bbrc.2012.11.108

supernatants from cells rendered defective for PML by RNA interference. The results provide evidence that PML is required for HCV production.

2. Materials and methods

2.1. Cell culture

293FT cells were cultured in Dulbecco's modified Eagle's medium (DMEM; Invitrogen, Carlsbad, CA, USA) supplemented with 10% fetal bovine serum (FBS). The three HuH-7-derived cell lines: RSc cured cells that cell culture-generated HCV-JFH1 (JFH1 strain of genotype 2a) [9] could infect and effectively replicate [10–13], OR6c cells is cured cells of OR6 cells harboring the genome-length HCV-O RNA with luciferase as a reporter [14] or OR6c JRN/3-5B cells harboring the subgenome HCV-JFH1 RNA with luciferase as a reporter were cultured in DMEM with 10% FBS as described previously [13].

2.2. RNA interference

Oligonucleotides with the following sense and antisense sequences were used for the cloning of short hairpin RNA (shRNA)-encoding sequences targeted to DDX5 in a lentiviral vector: 5′-GATCCCCCTCTAATGTGGAGTGCGACTTCAAGAGAGTCGCACTCCACA TTAGAGTTTTTGGAAA-3′ (sense), 5′-AGCTTTTCCAAAAACTCTAATGT GGAGTGCGACTCTCTTGAAGTCGCACTCCACATTAGAGGGG-3′ (antisense). The oligonucleotides above were annealed and subcloned into the *Bgl*II-*Hin*dIII site, downstream from an RNA polymerase III promoter of pSUPER [15], to generate pSUPER-DDX5i. To construct pLV-DDX5i, the *Bam*HI-*Sal*I fragments of the pSUPER-DDX5i were subcloned into the *Bam*HI-*Sal*I site of pRDI292, an HIV-1-derived self-inactivating lentiviral vector containing a puromycin resistance marker allowing for the selection of transduced cells [16]. We previously described pLV-PMLi [8] and pLV-INI1i [17], respectively.

2.3. Lentiviral vector production

The vesicular stomatitis virus (VSV)-G-pseudotyped HIV-1-based vector system has been described previously [18,19]. The lentiviral vector particles were produced by transient transfection of the second-generation packaging construct pCMV-ΔR8.91 [18,19] and the VSV-G-envelope-expressing plasmid pMDG2 as well as pLV-PMLi into 293FT cells with FuGene6 (Roche Diagnostics, Mannheim, Germany).

2.4. HCV infection experiments

The supernatants was collected from cell culture-generated HCV-JFH1-infected RSc cells at 5 days post-infection and stored at −80 °C after filtering through a 0.45 μm filter (Kurabo, Osaka, Japan) until use. For infection experiments with HCV-JFH1 virus or J6/JFH1 [20], RSc cells (5×10^4 cells/well) were plated onto 6-well plates and cultured for 24 h (hrs). We then infected the cells at a multiplicity of infection (MOI) of 0.05. The culture supernatants were collected at the indicated time post-infection and the levels of the core protein were determined by enzyme-linked immunosorbent assay (Mitsubishi Kagaku Bio-Clinical Laboratories, Tokyo, Japan). Total RNA was isolated from the infected cellular lysates using RNeasy mini kit (Qiagen, Hilden, Germany) for quantitative RT-PCR analysis of intracellular HCV RNA. The infectivity of HCV-JFH1 in the culture supernatants was determined by a focus-forming assay at 48 h post-infection.

2.5. Quantitative RT-PCR analysis

The quantitative RT-PCR analysis for HCV RNA was performed by real-time LightCycler PCR (Roche) as described previously [14]. We used the following forward and reverse primer sets for the real-time LightCycler PCR: PML, 5′-GAGGAGTTCCAGTTTCT GCG-3′ (forward), 5′-GCGCCTGGCAGATGGGGCAC-3′ (reverse); DDX5, 5′-ATGTCGGGTTATTCGAGTGA-3′ (forward), 5′-TTTCTCC CCAGGGTTTCCAA-3′ (reverse); INI1, 5′-ATGATGATGATGGCGCTG AG-3′ (forward), 5′-TCGGAACATACGGAGGTAGT-3′ (reverse); β-actin, 5′-TGACGGGGTCACCCACACTG-3′ (forward), 5′-AAGCTGTAG CCGCGCTCGGT-3′ (reverse); and HCV-JFH1, 5′-AGAGCCATAGTGGT CTGCGG-3′ (forward), 5′-CTTTCGCAACCCAACGCTAC-3′ (reverse).

2.6. Western blot analysis

Cells were lysed in buffer containing 50 mM Tris–HCl (pH 8.0), 150 mM NaCl, 4 mM EDTA, 1% Nonidet P-40, 0.1% sodium dodecyl sulfate (SDS), 1 mM dithiothreitol and 1 mM phenylmethylsulfonyl fluoride. Supernatants from these lysates were subjected to SDS–polyacrylamide gel electrophoresis, followed by immunoblot analysis using anti-HCV core (CP-9 and CP-11; Institute of Immunology, Tokyo, Japan) or anti-β-actin antibody (Sigma).

2.7. WST-1 assay

RSc or OR6c JRN/3-5B cells (1×10^3 cells/well) were plated onto 96-well plates and cultured. The cells were subjected to the WST-1 cell proliferation assay (Takara Bio, Otsu, Japan) according to the manufacturer's protocol. The absorbance was read using a microplate reader at 440 nm with a reference wavelength of 690 nm.

2.8. Renilla luciferase (RL) assay

OR6c JRN/3-5B cells (1.5×10^4 cells/well) were plated onto 24-well plates and cultured for 72 h, then, subjected to the RL assay according to the manufacturer's instructions (Promega, Madison, WI, USA). A lumat LB9507 luminometer (Berthold, Bad Wildbad, Germany) was used to detect RL activity.

2.9. RNA synthesis and transfection

Plasmid pJRN/3-5B was linearized by digestion with *Xba*I and was used for RNA synthesis with T7 MEGAscript (Ambion) as previously described [13]. *In vitro* transcribed RNA was transfected into OR6c cells by electroporation as described previously [14].

2.10. Immunofluorescence and confocal microscopic analysis

Cells were fixed in 3.6% formaldehyde in phosphate-buffered saline (PBS), permeabilized in 0.1% Nonidet P-40 in PBS at room temperature, and incubated with anti-PML antibody (PM001, MBL) and anti-HCV core at a 1:300 dilution in PBS containing 3% bovine serum albumin (BSA) at 37 °C for 30 min. They were then stained with anti-Cy3-conjugated anti-mouse antibody (Jackson ImmunoResearch, West Grove, PA) or Alexa Fluor 647-conjugated anti-rabbit antibody (Molecular Probes, Invitrogen) at a 1:300 dilution in PBS containing BSA at 37 °C for 30 min. Lipid droplets and nuclei were stained with BODIPY 493/503 (Molecular Probes, Invitrogen) and DAPI (4′, 6′-diamidino-2-phenylindole), respectively. Following extensive washing in PBS, the cells were mounted on slides using a mounting media of SlowFade Gold antifade reagent (Invitrogen) added to reduce fading. Samples were viewed under a confocal laser-scanning microscope (FV1000; Olympus, Tokyo, Japan).

3. Results

3.1. PML is involved in the propagation of HCV

To investigate the potential role(s) of PML in HCV life cycle, we first used lentiviral vector-mediated RNA interference to stably knockdown PML in HuH-7-derived RSc cured cells that HCV-JFH1 [9] could infect and effectively replicate [10–13]. Real-time RT-PCR analysis for PML demonstrated a very effective knockdown of PML in RSc cells transduced with lentiviral vector expressing shRNA targeted to PML (Fig. 1A). To test the cell toxicity of shRNA, we examined WST-1 assay. In spite of very effective knockdown of PML, we demonstrated that the shRNA targeted to PML did not affect the cell viabilities (Fig. 1B). We next examined the level of secreted HCV core and the infectivity of HCV in the culture supernatants as well as the level of HCV RNA in PML knockdown RSc cells 24, 48, or 72 h after HCV-JFH1 infection at an MOI of 0.05. The results showed that the level of HCV RNA in PML knockdown cells was not affected until 72 h post-infection (Fig. 1C), while the release of HCV core protein into the culture supernatants was significantly suppressed in PML knockdown cells at 48 or 72 h post-infection (Fig. 1D). Consistent with this finding, the infectivity of HCV in the culture supernatants was also significantly suppressed in the PML knockdown cells at 48 or 72 h post-infection (Fig. 1E). We also obtained similar results using siRNA specific for human PML (siGENOME SMRT pool M-006547-01-0005, Dharmacon, Thermo Fisher Scientific, Waltham, MA) (data not shown). These results suggested that PML is associated with propagation of HCV.

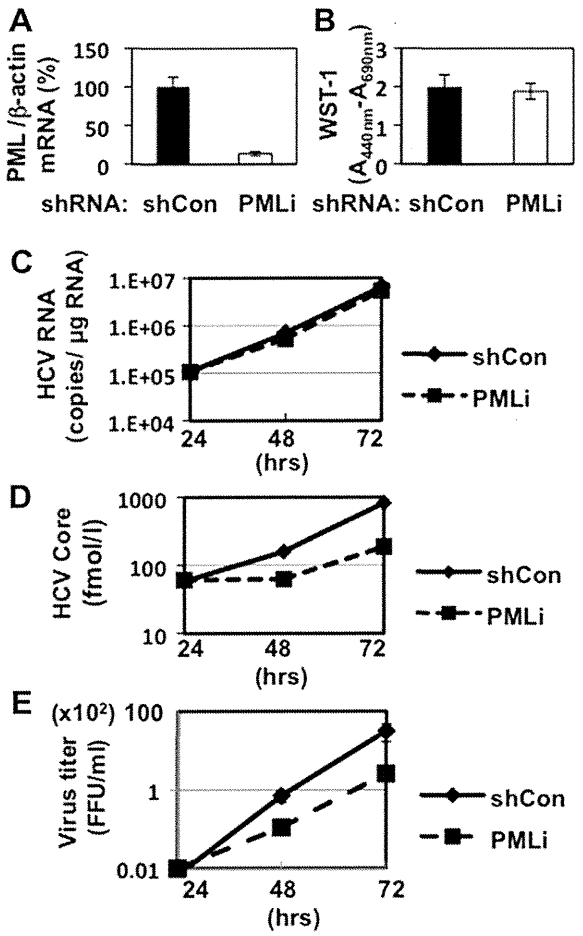

Fig. 1. PML is required for infectious HCV production. (A) Inhibition of PML mRNA expression by the shRNA-producing lentiviral vector. Real-time LightCycler RT-PCR for PML was performed as well as for β-actin mRNA. Each mRNA level was calculated relative to the level in RSc cells transduced with a control lentiviral vector (shCon) which was assigned as 100%. (B) WST-1 assay of the PML knockdown (PMLi) or the control (shCon) RSc cells. (C) The levels of intracellular genome-length HCV-JFH1 RNA in the PML knockdown or the control cells at 24, 48 or 72 h post-infection at an MOI of 0.05 were monitored by real-time LightCycler RT-PCR. (D) The levels of HCV core in the culture supernatants from the PML knockdown or the control RSc cells 24, 48 or 72 h after inoculation of HCV-JFH1 were determined by ELISA. (E) The infectivity of HCV in the culture supernatants was determined by a focus-forming assay at 48 h post-infection. All experiments were done in triplicate.

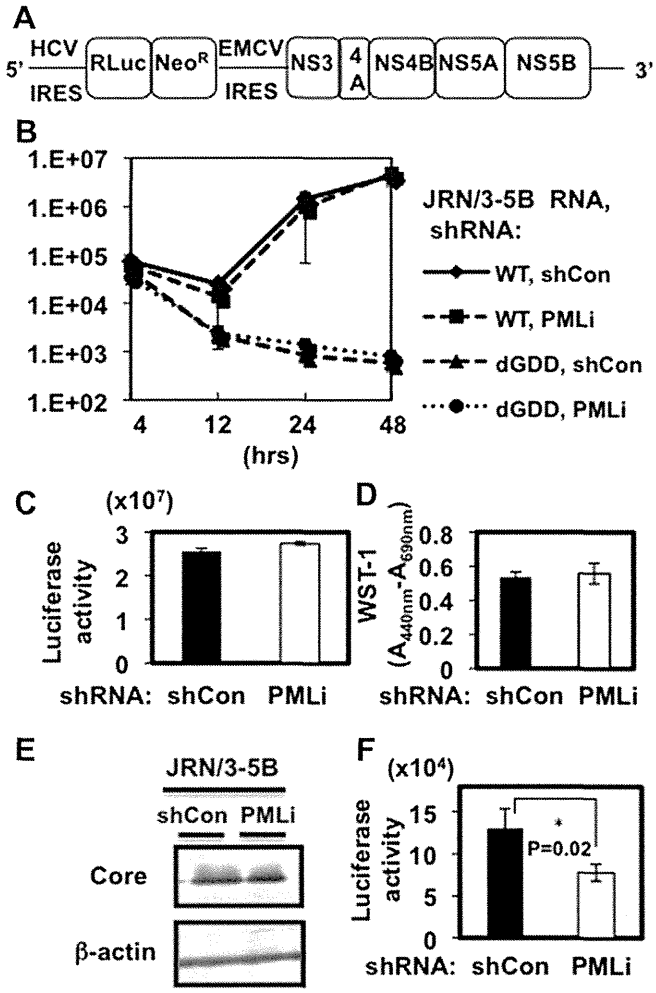

Fig. 2. PML is unrelated to the HCV RNA replication. Schematic gene organization of subgenomic JFH1 (JRN/3-5B) RNA encoding *Renilla* luciferase (RL) gene. *Renilla* luciferase gene (RLuc) is depicted as a box and is expressed as a fusion protein with Neo. (B) The transient replication of subgenomic HCV-JFH1 replicon in the PML knockdown (PMLi) or the control OR6c cells (shCon) after electroporation of *in vitro* transcribed JRN/3-5B RNA (10 μg) was monitored by RL assay at the indicated time. The results of *Renilla* luciferase activity are shown. dGDD indicates the deletion of the GDD motif in the NS5B polymerase, and the subgenomic HCV replicon with the deletion of GDD was used as a negative control. (C) The level of HCV RNA replication in PML knockdown (PMLi) or the control (shCon) OR6c JRN/3-5B cells was monitored by RL assay. The results shown are means from three independent experiments. (D) WST-1 assay of the PML knockdown or the control JRN/3-5B cells. (E) The level of HCV core protein in OR6c JRN/3-5B cells by expression of HCV core to NS2 coding region of HCV-JFH1 using mouse retroviral vector. pCX4bsr-JFH1-myc-C-NS2 and pMDG2 were cotransfected into Plat-E cells, mouse retroviral packaging cells. Mouse retroviral vector was obtained from their culture supernatants and transduced into OR6c JRN/3-5B PML knockdown or the control cells. The results of Western blot analysis of cellular lysates with anti-HCV core or an anti β-actin antibody are shown. (F) The level of HCV RNA replication in RSc cells 72 h after inoculation of HCV-like particles produced using *trans*-packaging system was monitored by RL assay. Asterisk indicates significant difference compared to the control. *$P = 0.02$.